

## ResearchSpace@Auckland

### Journal Article Version

This is the publisher's version. This version is defined in the NISO recommended practice RP-8-2008 <http://www.niso.org/publications/rp/>

### Suggested Reference

Wang, S. (2008). A novel method for analyzing the global stability of inviscid columnar swirling flow in a finite pipe. *Physics of Fluids*, 20(7).  
doi:10.1063/1.2939389

### Copyright

Copyright 2008 American Institute of Physics. This article may be downloaded for personal use only. Any other use requires prior permission of the author and the American Institute of Physics.

Items in ResearchSpace are protected by copyright, with all rights reserved, unless otherwise indicated. Previously published items are made available in accordance with the copyright policy of the publisher.

<http://www.sherpa.ac.uk/romeo/issn/1070-6631/>

<https://researchspace.auckland.ac.nz/docs/uoa-docs/rights.htm>

## A novel method for analyzing the global stability of inviscid columnar swirling flow in a finite pipe

S. Wang

Citation: [Phys. Fluids](#) **20**, 074101 (2008); doi: 10.1063/1.2939389

View online: <http://dx.doi.org/10.1063/1.2939389>

View Table of Contents: <http://pof.aip.org/resource/1/PHFLE6/v20/i7>

Published by the [American Institute of Physics](#).

---

### Related Articles

Fluid flows in a librating cylinder

[Phys. Fluids](#) **24**, 026603 (2012)

Mobility matrix of a spherical particle translating and rotating in a viscous fluid confined in a spherical cell, and the rate of escape from the cell

[J. Chem. Phys.](#) **136**, 054703 (2012)

Dipole evolution in rotating two-dimensional flow with bottom friction

[Phys. Fluids](#) **24**, 026602 (2012)

Negative Magnus lift on a rotating sphere at around the critical Reynolds number

[Phys. Fluids](#) **24**, 014102 (2012)

Three-dimensional swirling flows in a tall cylinder driven by a rotating endwall

[Phys. Fluids](#) **24**, 014101 (2012)

---

### Additional information on Phys. Fluids

Journal Homepage: <http://pof.aip.org/>

Journal Information: [http://pof.aip.org/about/about\\_the\\_journal](http://pof.aip.org/about/about_the_journal)

Top downloads: [http://pof.aip.org/features/most\\_downloaded](http://pof.aip.org/features/most_downloaded)

Information for Authors: <http://pof.aip.org/authors>

### ADVERTISEMENT



## Running in Circles Looking for the Best Science Job?

Search hundreds of exciting  
new jobs each month!

<http://careers.physicstoday.org/jobs>

physicstodayJOBS



# A novel method for analyzing the global stability of inviscid columnar swirling flow in a finite pipe

S. Wang<sup>a)</sup>

Department of Mathematics, Auckland University, Private Bag 92019, Auckland 1142, New Zealand

(Received 17 March 2008; accepted 6 May 2008; published online 1 July 2008)

We developed a general strategy to study the stability problem of the inviscid columnar swirling flow in a finite pipe based on the perturbation method of linear operators. By virtue of the columnar base state, we were able to derive all the necessary formulas used in perturbation method in a manner of separation of variables. We then conduct a necessary benchmark case study based on the solid body rotation flow. We then applied the general method to the Lamb–Oseen vortex and the  $q$ -vortex and found their approximated growth rate functions. The perturbation method proved effective and robust in application to these vortex flows. We also extended the method by using the analytic continuation to find the unstable modes with complex growth rates. This analytic continuation method reflects the global nature of the perturbation method. Using the new method, we investigated the energy transfer mechanism of the Lamb–Oseen vortex in a finite pipe and revealed a new energy transfer mechanism related to the flow stability. © 2008 American Institute of Physics. [DOI: 10.1063/1.2939389]

## I. INTRODUCTION

The study of the stability of an axisymmetric and swirling flow in a pipe goes back to Rayleigh's milestone work<sup>1</sup> in 1916. Rayleigh established a fundamental stability criterion for swirling flows in an infinitely long straight pipe. Rayleigh's criterion states that a columnar swirling flow with a swirl velocity component  $V(r)$  and uniform axial velocity components is stable to infinitesimal axisymmetric disturbances if and only if the square of the circulation function,  $K=rV$ , decreases nowhere as  $r$  increases from the center of the pipe to the pipe wall, i.e.,

$$\Phi \equiv \frac{1}{r^3} \frac{d}{dr} (K^2) \geq 0. \quad (1)$$

Notice that the necessity and sufficiency of Eq. (1) for swirling flow being stable are strongly tied with the assumption imposed on the base swirling flow, namely, a columnar swirling flow in an infinite pipe. Such flows apparently preserve a translation invariance and therefore admit a Fourier mode analysis without losing any generality. It has since become a common practice in the study of the stability to assume that the flow is uniform in the axial direction. Technically, this often reduces the task to solve an eigenvalue problem with only ordinary differential equations involved. However, in a real problem, flows are often seen having significant spatial development and under strong upstream and down stream influence. Applying the Rayleigh criterion to these flows could be questionable.

In the study of vortex breakdown in a finite pipe, the influence of the physical conditions at pipe inlet and outlet has been studied by Wang and Rusak.<sup>2,3</sup> It was found that the boundary conditions imposed dramatically alter the stability nature of the swirling flow. In particular, an instability related

to the swirl strength was found that cannot be explained by Rayleigh's stability theory. This type of stability has been aptly interpreted by Gallaire and Chomaz<sup>4</sup> as being *global* in nature. There, we will use the *global stability* to denote this type of stability.

The global instability which occurs at high swirl is found to be in good correlation with the experimental observations. In experiments (see, for example, Garg and Leibovich<sup>5</sup>) it has been observed that the swirl ratio, which is defined as the ratio of the circumferential and axial velocities, can predict the occurrence of vortex breakdown with certain degree of success. Recent experiment of Mattner *et al.*<sup>6</sup> has showed that the occurrence of bubble-type vortex breakdown can be predicted by Wang and Rusak's global bifurcation diagram,<sup>2</sup> which is closely related to the global stability. For further revealing the role of the global stability in vortex breakdown phenomenon, one must compare the actual flow transition to the prediction of the stability theory. This raises the need for analyzing the global stability of the swirling flows of interest.

Currently, only one flow model has been thoroughly studied in this aspect, namely, the solid body rotation flow: A column of fluid moving at a constant axial velocity and rotating in a solid body. For this particular model the stability equation can be analytically solved by separating variables since the axial and radial disturbances in the case can be completely decoupled. However, this method does not fit to solve stability problems for more realistic swirling flows such as the Lamb–Oseen vortex and  $q$ -vortex. We will develop a new method in this article to solve the stability problem for an arbitrarily given columnar swirling flow. The method is based on the perturbation theory of the linear operators. The stability problem can be written as an eigenvalue problem of a perturbed linear operator. With this formulation, we may exploit the power of the perturbation theory of

<sup>a)</sup>Electronic mail: wang@math.auckland.ac.nz.

linear operators and solve the stability problem in a general manner.

We first develop the techniques for treating the stability problem of general columnar swirling flows. By virtue of the columnar base state, we show that all the analysis can be done in a manner of separation of variables, a crucial fact to ensure the method effective. We are then able to show a general approach to solve the global stability problem for given columnar states. The necessary perturbation theory of the linear operators is introduced in Appendix A.

We then conduct a *benchmark case study* based on the well studied flow model: *The solid body rotation flow*. Such a benchmark study is necessary. In the perturbation method, one finds and uses finite terms in a power series to approximate the true function. The effectiveness of the method is dependent on the good behavior of this series. Especially, fast convergence and sufficient large convergence radius are key to the success of the method. Through this benchmark study, we establish the effectiveness and correctness of the method and learn at the same time the general behaviors of the method.

We then apply the method to two important vortex flows, the Lamb–Oseen vortex and the  $q$ -vortex, and found their growth rate functions. Two types of boundary conditions have been considered: One with nonradial velocity at the outlet and the other with fixed flowrate at the outlet. The perturbation method proved effective and robust in application to these vortex flows. With low order approximation, of which the computation cost is negligible, a large part of the growth rate function can be accurately found in an algebraic form.

We extend the method by using the analytic continuation and thus find the unstable modes with complex growth rates. These are oscillating modes that exist in a specific range of swirl for all columnar swirling flows. An interesting feature in use of the analytic continuation is that one does not need to develop another expansion for the complex growth rate; instead, one simply makes use of the real growth rate function, extends it to the complex plane, and thereby finds the complex branch. These unstable oscillating modes are possible related to the observed oscillations of the vortex breakdown bubbles.

Through this study, we establish an effective and useful tool to study the global stability problem for the inviscid columnar swirling flow in a finite pipe. This fills a technical gap in the study of the dynamics of the swirling flow. At the end, as an application example, we show how to use the method to analyze the energy transfer mechanism of the Lamb–Oseen vortex in a finite pipe.

## II. THE STABILITY EQUATION FOR COLUMNAR SWIRLING FLOW

We consider axisymmetric, incompressible, and inviscid flows in a finite length pipe. We use cylindrical coordinates  $(r, \theta, x)$  and the velocity components  $(u, v, w)$  corresponding to the radial, azimuthal, and axial velocities, respectively. In the dimensionless form, the pipe radius is set as a unit and the pipe length as  $L$ , rescaled with respect to the pipe radius.

By virtue of the axisymmetry, the stream function  $\psi(x, r, t)$  can be defined such that  $u = -\psi_x/r$  and  $w = \psi_r/r$ . Let  $y = r^2/2$ , in terms of this new variable,  $w = \psi_y$ ,  $u = -\psi_x/\sqrt{2y}$ , and the reduced form of azimuthal vorticity  $\chi = -(\psi_{yy} + \psi_{xx}/2y)$  (the azimuthal vorticity  $\eta = \chi/r$ ).

The Euler equation in terms of  $\psi$ ,  $\chi$  and the circulation function  $K$ , defined as  $K = rv$ , can be written in a compact form (see, for example, Szeri and Holmes<sup>7</sup>),

$$K_t + \{\psi, K\} = 0, \quad (2)$$

$$\chi_t + \{\psi, \chi\} = \frac{1}{4y^2}(K^2)_x,$$

where the bracket  $\{f, g\}$  is the canonical Poisson bracket or Jacobian defined as

$$\{f, g\} = f_y g_x - f_x g_y. \quad (3)$$

For the steady state,  $\psi(x, y)$  satisfies the well-known steady Squire–Long equation, which can be derived from Eq. (2) (see Squire<sup>8</sup> and Long<sup>9</sup>),

$$\psi_{yy} + \frac{\psi_{xx}}{2y} = H'(\psi) - \frac{I'(\psi)}{2y}, \quad (4)$$

where  $H = p/\rho + (u^2 + v^2 + w^2)/2$  is the total head function ( $p$  is pressure and  $\rho$  is density) and  $I = K^2/2$  is the extended circulation, both of which are functions of  $\psi(x, y)$  only.

Throughout this article, we consider a steady, columnar swirling base flow with the velocity components specified by

$$(u, v, w) = [0, \omega v_0(y), w_0(y)], \quad (5)$$

where  $\omega > 0$  is the swirl parameter. From this velocity profile, one may find  $\psi_0(y) = \int_0^y w_0(y) dy$ ,  $\chi_0 = -(\psi_{0yy} + \psi_{0xx}/2y) = -w_{0y}(y)$ ,  $K = \omega K_0(y)$ , with  $K_0(y) = \sqrt{2y}v_0(y)$  and  $I = \omega^2 I_0$  with  $I_0 = K_0^2/2$ .

In the study of linear stability, disturbances of stream function  $\psi_1$  and circulation  $K_1$  are assumed in the forms

$$\psi_1(x, y, t) = \epsilon \phi(x, y) e^{\sigma t}, \quad (6)$$

$$K_1(x, y, t) = \epsilon k(x, y) e^{\sigma t},$$

with  $\epsilon \ll 1$ , where  $\sigma$  is in general a complex number that gives the growth rate. These disturbance terms are superimposed to the base flow state and substituted into the Euler equation (2). By neglecting the second order perturbation terms, one obtains

$$\left\{ \phi_{yy} + \frac{\phi_{xx}}{2y} - \left[ H''(\psi_0) - \frac{I''(\psi_0)}{2y} \right] \phi \right\}_{xx} + \frac{\sigma \chi_{0y}}{w_0^2} \phi_x + \frac{2\sigma}{w_0} \left( \phi_{yy} + \frac{\phi_{xx}}{2y} \right)_x + \frac{\sigma^2}{w_0^2} \left( \phi_{yy} + \frac{\phi_{xx}}{2y} \right) = 0. \quad (7)$$

For the detailed derivation of Eq. (7), see Wang and Rusak.<sup>3</sup> Equation (7) is the basic stability equation in this study. Notice that this equation can be used for columnar swirling flows with or without the axial shear ( $w_0(y)$  may not be constant).

The eigenvalue problem (7) shall be solved subject to a set of boundary conditions. We consider the boundary conditions same as in Wang and Rusak,<sup>3</sup>

$$\phi(x, 0) = 0, \quad \phi\left(x, \frac{1}{2}\right) = 0 \quad \text{for } 0 \leq x \leq L,$$

$$\phi(0, y) = 0, \quad \phi_{xx}(0, y) = 0, \quad k(0, y) = 0 \quad \text{for } 0 \leq y \leq \frac{1}{2}, \quad (8)$$

$$\phi_x(L, y) = 0 \quad \text{for } 0 \leq y \leq \frac{1}{2}.$$

Furthermore,  $k(0, y) = 0$  can be replaced by

$$\phi_{yyx}(0, y) + \frac{\phi_{xxx}(0, y)}{2y} - \left[ H''(\psi_0) - \frac{I''(\psi_0)}{2y} \right] \phi_x(0, y) = 0. \quad (9)$$

These boundary conditions specify a fixed  $K$ ,  $\chi$ , and  $w$  at the inlet and a fixed  $u$  at the outlet. We will also consider another set of boundary conditions later on.

### III. GENERAL APPROACH TO COLUMNAR SWIRLING FLOWS

In this section we will apply the perturbation method to study the stability equation of the columnar swirling flow. We derive the stability equation for a given columnar swirling flow and reformulate it as a perturbation problem. We then develop the detailed techniques to solve this perturbation problem. The perturbation method of linear operators is introduced in Appendix A.

#### A. The stability equation for a given flow state

In the stability equation, the term

$$H''(\psi_0) - \frac{I''(\psi_0)}{2y} \quad (10)$$

shall be determined from the given columnar flow state:  $\psi = \psi_0(y)$  and  $K = \omega K_0(y)$ . One has  $I = \omega^2 I_0(y)$  or  $I = \Omega I_0(y)$  by using a rescaled swirl parameter  $\Omega = \omega^2$ . We may write Eq. (10) as

$$H''(\psi_0; \Omega) - \frac{\Omega I_0''(\psi_0)}{2y}, \quad (11)$$

to indicate that  $H''(\psi_0; \Omega)$  is dependent on the parameter  $\Omega$ . From the Squire–Long equation (4), one obtains

$$\psi_{0yy} = w_{0y} = H'(\psi_0; \Omega) - \frac{\Omega I_0'(\psi_0)}{2y}. \quad (12)$$

By differentiating Eq. (12) with respect to  $y$ , one obtains

$$w_{0yy} = H''(\psi_0; \Omega) w_0 - \frac{\Omega I_0''(\psi_0) w_0}{2y} + \frac{\Omega I_0'(\psi_0)}{2y^2}, \quad (13)$$

which gives an explicit formula of Eq. (11) in terms of  $w_0$  and  $I_0$ ,

$$H''(\psi_0; \Omega) - \frac{\Omega I_0''(\psi_0)}{2y} = \frac{w_{0yy}}{w_0} - \frac{\Omega I_0'(\psi_0)}{2w_0 y^2}. \quad (14)$$

We may now write Eq. (7) explicitly in terms of the given columnar state

$$\left\{ \phi_{yy} + \frac{\phi_{xx}}{2y} - \left[ \frac{w_{0yy}}{w_0} - \frac{\Omega I_0'(\psi_0)}{2w_0 y^2} \right] \phi \right\}_{xx} - \frac{\sigma w_{0yy}}{w_0^2} \phi_x + \frac{2\sigma}{w_0} \left( \phi_{yy} + \frac{\phi_{xx}}{2y} \right)_x + \frac{\sigma^2}{w_0^2} \left( \phi_{yy} + \frac{\phi_{xx}}{2y} \right) = 0, \quad (15)$$

where one also uses the relation  $\chi_{0y} = -w_{0yy}$ .

We may define  $m(y)$  by

$$m(y) = \frac{2w_0 y^2}{I_0'(\psi_0)} = \frac{2w_0^2 y^2}{[I_0(\psi_0(y))]_y}, \quad (16)$$

provided that  $I_0[\psi_0(y)]_y$  nowhere vanishes in the interval  $(0, \frac{1}{2})$ .

Integrating Eq. (15) twice along the  $x$ -direction by using whichever boundary conditions (8) applicable and multiplying the entire equation with  $m(y)$ , the stability equation of the general columnar swirling flow is effectively written as a perturbation problem,

$$\begin{aligned} & \underbrace{-m(y) \left[ \left( \phi_{yy} + \frac{\phi_{xx}}{2y} \right) - \frac{w_{0yy}}{w_0} \phi \right]}_{T^{(0)}} \\ & + \underbrace{\sigma \int_0^x -m(y) \left[ \frac{2}{w_0} \left( \phi_{yy} + \frac{\phi_{xx}}{2y} \right) - \frac{w_{0yy}}{w_0^2} \right] dx}_{T^{(1)}} \\ & + \underbrace{\sigma^2 \int_0^x \int_0^x -\frac{m(y)}{w_0^2} \left( \phi_{yy} + \frac{\phi_{xx}}{2y} \right) dx dx}_{T^{(2)}} = \Omega \phi, \quad (17) \end{aligned}$$

which is subject to the boundary conditions left,

$$\phi(x, 0) = 0, \quad \phi(x, 1/2) = 0 \quad \text{for } 0 \leq x \leq L,$$

$$\phi(0, y) = 0 \quad \text{for } 0 \leq y \leq 1/2, \quad (18)$$

$$\phi_x(L, y) = 0 \quad \text{for } 0 \leq y \leq 1/2.$$

#### B. Solve the stability problem by using the perturbation method of linear operators

The stability problem can be written as a perturbed eigenvalue problem of a linear operator in the form

$$T(\sigma) \phi = \Omega \phi \quad \text{where } T(\sigma) = T^{(0)} + \sigma T^{(1)} + \sigma^2 T^{(2)}. \quad (19)$$

Notice that the growth rate  $\sigma$  appears in Eq. (19) as a given perturbation parameters, while the swirl parameter  $\Omega$  is the eigenvalue to be sought.

The key observation of this perturbation problem is that the unperturbed problem,

$$T^{(0)} \phi = \Omega \phi, \quad (20)$$

can be solved by the method of separation of variables for all columnar state. The eigenvalues of  $T^{(0)}$ , called as critical swirls, correspond to the special flow states where neutral modes exist. At the critical swirl  $\Omega_c$ , the growth rate  $\sigma = 0$ , and one seeks the following expansion:

$$\Omega = \Omega_c + \sum_{n=1}^{\infty} c_n \sigma^n. \quad (21)$$

In the perturbation theory it can be proved that the formal expansion actually converges to an analytic function in a disk in the complex plane. Technically, all the coefficients in the expansion (21) can be found from the operators  $T^{(0)}$ ,  $T^{(1)}$ , and  $T^{(2)}$  in a systematic way. In Appendix A, we present the perturbation theory and show how to apply it to the stability problem. In particular, explicit formulas for evaluating the coefficients are given. From this appendix, we found the following steps to perform the perturbation method.

- (1) Find a proper inner product such that the unperturbed operator  $T^{(0)}$  is symmetric about this inner product and solve the eigenvalue problem for  $T^{(0)}$ .
- (2) Find special inner products involved with the eigenfunctions found in previous step and the operators  $T^{(1)}$  and  $T^{(2)}$ .
- (3) Evaluate the coefficients in the expansion by using the formulas derived from the perturbation method.

Each of them will be carefully addressed in the following. In the evaluation of the coefficients, we have taken the full advantage of the columnar state and do whatever possible analytic work to simplify the method. At the end, we obtain a set of formulas to perform the perturbation method for stability problem. These formulas are general and ready to be applied to various vortex flows.

### 1. The analysis of the operator $T^{(0)}$

Consider the unperturbed eigenvalue problem for  $T^{(0)}$ ,

$$-m(y) \left[ \left( \phi_{yy} + \frac{\phi_{xx}}{2y} \right) - \frac{w_{0yy}}{w_0} \phi \right] = \Omega \phi, \quad (22)$$

subject to the boundary conditions (18). The proper Hilbert space of this problem is  $L^2_{1/m(y)}(D)$ , the  $1/m(y)$  weighted square integrable function space on the domain  $D=(0,L) \times (0, \frac{1}{2})$  with the inner product defined as

$$(\phi_1, \phi_2) = \int_D \frac{\phi_1(x,y) \phi_2(x,y)}{m(y)} dx dy. \quad (23)$$

$T^{(0)}$  is a symmetric operator, namely, by integrating in parts,

$$\begin{aligned} \int_D \frac{(T^{(0)}\phi)\psi}{m(y)} dx dy &= \int_D \left( \phi_{yy} + \frac{\phi_{xx}}{2y} - \frac{w_{0yy}}{w_0} \phi \right) \psi dx dy \\ &= \int_D \left( \psi_{yy} + \frac{\psi_{xx}}{2y} - \frac{w_{0yy}}{w_0} \psi \right) \phi dx dy \\ &= \int_D \frac{(T^{(0)}\psi)\phi}{m(y)} dx dy. \end{aligned} \quad (24)$$

The normalized eigenfunctions of Eq. (22) denoted by  $\phi_{o,n}^*(x,y)$  can be found as

$$\phi_{o,n}^*(x,y) = \sqrt{\frac{2}{L}} \Phi_{o,n}^*(y) \sin \left[ \frac{(2n-1)\pi x}{2L} \right], \quad (25)$$

with  $\Phi_{o,n}^*(y)$  solving the reduced zeroth order eigenvalue problem

$$\Phi_{yy} - \frac{(2n-1)^2 \pi^2 \Phi}{8L^2 y} + \left( \frac{\Omega_{o,n}}{m(y)} - \frac{w_{0yy}}{w_0} \right) \Phi = 0, \quad (26)$$

$$\Phi(0) = 0, \quad \Phi\left(\frac{1}{2}\right) = 0,$$

and normalized as

$$\left[ \int_0^{0.5} \frac{\Phi_{o,n}^{*2}(y)}{m(y)} dy \right]^{1/2} = 1, \quad (27)$$

where  $\Omega_{o,n}$  are eigenvalues with  $o=1,2,3,\dots$  and  $n=1,2,3,\dots$  in the order  $\Omega_{o_1,n_1} \leq \Omega_{o_2,n_2}$  for  $o_1 \leq o_2$  and  $n_1 \leq n_2$ .

### 2. The analysis of $(T^{(1)}\phi_{o_1,m}^*, \phi_{o_2,n}^*)$ and $(T^{(2)}\phi_{o_1,m}^*, \phi_{o_2,n}^*)$

Two types of inner products  $(T^{(1)}\phi_{o_1,m}^*, \phi_{o_2,n}^*)$  and  $(T^{(2)}\phi_{o_1,m}^*, \phi_{o_2,n}^*)$  must be evaluated before further proceeding of the method. According to the definition of  $T^{(1)}$  and  $T^{(2)}$ , one has

$$\begin{aligned} T^{(1)}\phi_{o,n}^* &= - \int_0^x \frac{2m(y)}{w_0} \left[ (\phi_{o,n}^*)_{yy} + \frac{(\phi_{o,n}^*)_{xx}}{2y} - \frac{w_{0yy}}{2w_0} \phi_{o,n}^* \right] dx \\ &= \frac{2m(y)}{w_0} \left( \frac{\Omega_{o,n}}{m(y)} - \frac{w_{0yy}}{2w_0} \right) \int_0^x \phi_{o,n}^* dx \\ &= \frac{2m(y)}{w_0} \left( \frac{\Omega_{o,n}}{m(y)} - \frac{w_{0yy}}{2w_0} \right) \Phi_{o,n}^*(y) \\ &\quad \times \int_0^x \sqrt{\frac{2}{L}} \sin \left[ \frac{(2n-1)\pi x}{2L} \right] dx, \end{aligned} \quad (28)$$

$$\begin{aligned} T^{(2)}\phi_{o,n}^* &= - \int_0^x dx \int_0^x \frac{m(y)}{w_0^2} \left[ (\phi_{o,n}^*)_{yy} + \frac{(\phi_{o,n}^*)_{xx}}{2y} \right] dx \\ &= \frac{m(y)}{w_0^2} \left[ \frac{\Omega_{o,n}}{m(y)} - \frac{w_{0yy}}{w_0} \right] \int_0^x dx \int_0^x \phi_{o,n}^* dx \\ &= \frac{m(y)}{w_0^2} \left[ \frac{\Omega_{o,n}}{m(y)} - \frac{w_{0yy}}{w_0} \right] \Phi_{o,n}^*(y) \\ &\quad \times \int_0^x dx \int_0^x \sqrt{\frac{2}{L}} \sin \left[ \frac{(2n-1)\pi x}{2L} \right] dx. \end{aligned} \quad (29)$$

We find that  $T^{(1)}\phi_{o,n}^*$  and  $T^{(2)}\phi_{o,n}^*$  are written in a form with the variables separated. Moreover, the  $x$ -dependent functions are but simple trigonometric functions and can be integrated. By substituting Eqs. (28) and (29) into  $(T^{(1)}\phi_{o_1,m}^*, \phi_{o_2,n}^*)$  and  $(T^{(2)}\phi_{o_1,m}^*, \phi_{o_2,n}^*)$ , respectively, one finds that the following integrals appear in the expression:

$$I_1(m, n) = \int_0^L \sqrt{\frac{2}{L}} \sin\left[\frac{(2n-1)\pi x}{2L}\right] \times \left\{ \int_0^x \sqrt{\frac{2}{L}} \sin\left[\frac{(2m-1)\pi x}{2L}\right] dx \right\} dx \quad (30)$$

$$I_2(m, n) = \int_0^L \sqrt{\frac{2}{L}} \sin\left[\frac{(2n-1)\pi x}{2L}\right] \times \left\{ \int_0^x dx \int_0^x \sqrt{\frac{2}{L}} \sin\left[\frac{(2m-1)\pi x}{2L}\right] dx \right\} dx. \quad (31)$$

and

In Appendix B, these integrals are found, by integration, as

$$I_1(m, n) = \begin{cases} \frac{8L}{(2m-1)^2 \pi^2} & \text{if } n = m, \\ \frac{4L}{(2m-1)\pi^2} \left[ \frac{4}{(2n-1)} + \frac{(-1)^{(n+m-1)} - 1}{(n+m-1)} + \frac{(-1)^{(n-m)} - 1}{(n-m)} \right] & \text{if } n \neq m, \end{cases} \quad (32)$$

and

$$I_2(m, n) = \begin{cases} \frac{4L^2}{\pi^3} \left[ \frac{-\pi}{(2m-1)^2} + \frac{4(-1)^{m+1}}{(2m-1)^3} \right] & \text{if } n = m, \\ \frac{(-1)^{n+1} 16L^2}{(2n-1)^2 (2m-1) \pi^3} & \text{if } n \neq m. \end{cases} \quad (33)$$

These functions reflect the influence of axial disturbance. By using these expressions, one obtains

$$(T^{(1)} \phi_{o_1, m}^*, \phi_{o_2, n}^*) = I_1(m, n) \left[ \Omega_{o_1, m} (\Phi_{o_1, m}^*, \Phi_{o_2, n}^*)_1 - \frac{1}{2} (\Phi_{o_1, m}^*, \Phi_{o_2, n}^*)_2 \right], \quad (34)$$

$$(T^{(2)} \phi_{o_1, m}^*, \phi_{o_2, n}^*) = I_2(m, n) \left[ \Omega_{o_1, m} (\Phi_{o_1, m}^*, \Phi_{o_2, n}^*)_3 - (\Phi_{o_1, m}^*, \Phi_{o_2, n}^*)_4 \right],$$

where

$$(\Phi_{o_1, m}^*, \Phi_{o_2, n}^*)_1 = \int_0^{1/2} \frac{\Phi_{o_1, m}^* \Phi_{o_2, n}^*}{m(y) w_0} dy, \quad (35)$$

$$(\Phi_{o_1, m}^*, \Phi_{o_2, n}^*)_2 = \int_0^{1/2} \frac{w_{0yy}}{w_0^2} \Phi_{o_1, m}^* \Phi_{o_2, n}^* dy,$$

$$(\Phi_{o_1, m}^*, \Phi_{o_2, n}^*)_3 = \int_0^{1/2} \frac{\Phi_{o_1, m}^* \Phi_{o_2, n}^*}{m(y) w_0^2} dy,$$

$$(\Phi_{o_1, m}^*, \Phi_{o_2, n}^*)_4 = \int_0^{1/2} \frac{w_{0yy}}{w_0^3} \Phi_{o_1, m}^* \Phi_{o_2, n}^* dy.$$

It is interesting to observe that when the axial shear is not present,

$$(\Phi_{o_1, m}^*, \Phi_{o_2, n}^*)_2 = \int_0^{1/2} \frac{w_{0yy}}{w_0^2} \Phi_{o_1, m}^* \Phi_{o_2, n}^* dy = 0, \quad (36)$$

$$(\Phi_{o_1, m}^*, \Phi_{o_2, n}^*)_4 = \int_0^{1/2} \frac{w_{0yy}}{w_0^3} \Phi_{o_1, m}^* \Phi_{o_2, n}^* dy = 0.$$

Moreover, Eq. (34) reduces to

$$(T^{(1)} \phi_{o_1, m}^*, \phi_{o_2, n}^*) = \Omega_{o_1, m} I_1(m, n) (\Phi_{o_1, m}^*, \Phi_{o_2, n}^*)_1, \quad (37)$$

$$(T^{(2)} \phi_{o_1, m}^*, \phi_{o_2, n}^*) = \Omega_{o_1, m} I_2(m, n) (\Phi_{o_1, m}^*, \Phi_{o_2, n}^*)_3.$$

The influence of the axial shear is partially represented by the terms of  $(\Phi_{o_1, m}^*, \Phi_{o_2, n}^*)_2$  and  $(\Phi_{o_1, m}^*, \Phi_{o_2, n}^*)_4$ . Note that the axial shear also affects the reduced zeroth order eigenvalue problem as a term  $-w_{0yy}/w_0$  that appears in Eq. (17).

### 3. Find the coefficients in the expansion

With this preparation, we are ready to apply the perturbation method. At each critical swirl  $\Omega_{o, m}$ , let  $\Delta_{o, m} \Omega(\sigma)$  be the swirl increment as a function of  $\sigma$ . The actual swirl can then be written in terms of  $\Delta_{o, m} \Omega(\sigma)$  as

$$\Omega = \Omega_{o, m} + \Delta_{o, m} \Omega(\sigma). \quad (38)$$

The perturbation theory of linear operators claims that the function  $\Delta_{o, m} \Omega(\sigma)$  is analytic in a complex disk, and has a power series expansion,

$$\Delta_{o, m} \Omega(\sigma) = \Omega_{o, m}^{(1)} \sigma + \Omega_{o, m}^{(2)} \sigma^2 + \Omega_{o, m}^{(3)} \sigma^3 + \dots \quad (39)$$

The coefficients in the power series are explicitly given by

$$\begin{aligned}
\Omega_{o,m}^{(1)} &= (T^{(1)} \phi_{o,m}^*, \phi_{o,m}^*), \\
\Omega_{o,m}^{(2)} &= (T^{(2)} \phi_{o,m}^*, \phi_{o,m}^*) \\
&- \sum_{o_1,n:(o_1,n) \neq (o,m)} \frac{(T^{(1)} \phi_{o,m}^*, \phi_{o_1,n}^*)(T^{(1)} \phi_{o_1,n}^*, \phi_{o,m}^*)}{\Omega_{o_1,n} - \Omega_{o,m}}.
\end{aligned} \quad (40)$$

In Appendix A one may find the general method to derive  $\Omega_{o,m}^{(n)}$ ,  $n=3,4$ .

We have found that the general columnar swirling flows with or without axial shear are all suitable to be analyzed by the linear operator perturbation method. The key observation is that the unperturbed operator  $T^{(0)}$ , and its interaction to the perturbed operators  $T^{(1)}$  and  $T^{(2)}$ , can all be analyzed by the method of separation of variable by virtue of the columnar base state. Notice that the original stability equation cannot be analyzed by the method of separation of variables with the only exception of the solid body rotation flow case. The perturbation method actually breaks up the whole problem into subproblems, each of which can be readily analyzed by the method of separation of variables.

#### IV. A BENCHMARK CASE STUDY WITH THE SOLID BODY ROTATION FLOW

The solid body rotation flow is defined as a column of fluid flowing at constant axial velocity  $w_0(r) \equiv W_0$  and solid body rotation  $v_0(r) = \omega r$  and  $u_0(r) = 0$ , where  $\omega$  is the swirl parameter. For this flow, assuming  $W_0 = 1$ , the stability equation (7) takes a particular simple form,

$$\begin{aligned}
\left( \phi_{yy} + \frac{\phi_{xx}}{2y} + \frac{\Omega}{2y} \phi \right)_{xx} + 2\sigma \left( \phi_{yy} + \frac{\phi_{xx}}{2y} \right)_x \\
+ \sigma^2 \left( \phi_{yy} + \frac{\phi_{xx}}{2y} \right) = 0,
\end{aligned} \quad (41)$$

where  $\Omega = 4\omega^2$  is a rescaled swirl parameter. Carefully examining this equation, one can find that all terms except  $\phi_{yy}$  have a common factor  $1/2y$ . This makes it possible to be solved by the method of separation of variables. For the detailed analysis, we refer to Wang and Rusak<sup>3</sup> and Gallaire and Chomaz.<sup>4</sup> As a well studied case with an accurate growth rate function available, the solid body rotation flow serves as an ideal vortex model for us to conduct a benchmark case study of the new method, a necessary task for validating the new approach.

By using the perturbation method, the stability equation takes the form

$$\begin{aligned}
\left( \phi_{yy} + \frac{\phi_{xx}}{2y} + \frac{\Omega}{2y} \phi \right) + \sigma \int_0^x 2 \left( \phi_{yy} + \frac{\phi_{xx}}{2y} \right) dx \\
+ \sigma^2 \int_0^x \int_0^x \left( \phi_{yy} + \frac{\phi_{xx}}{2y} \right) dx dx = 0.
\end{aligned} \quad (42)$$

The growth rates of the solid body rotation flow have been computed for a concrete case where the pipe length is  $L = 10$ . We now examine the first and second branches of approximations. Figure 1 shows the results from first order to fourth order approximation.

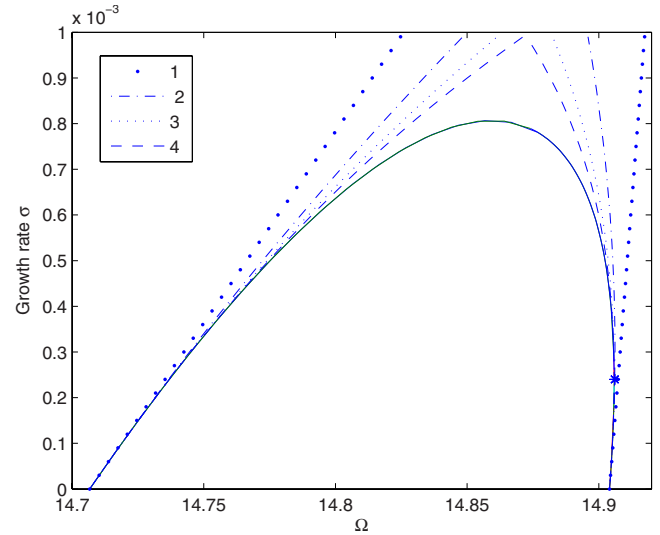


FIG. 1. (Color online) First to fourth order approximations of the growth rate curves between first and second critical swirls. The solid curve indicates the exact solution. The asterisk is the branching point.

We find the following from this plot.

- (1) The first order approximation is good only in a small  $\sigma$  range, about  $\sigma < 0.0001$ , and the second to fourth order approximations extend this range up to  $\sigma = 0.0005$ . Note that  $\sigma_{\max} \approx 0.0008$ .
- (2) The approximation captures some global nature of the growth rate function. For example, in the second branch of approximation the growth rate curve has a branching point at  $(\sigma^*, \Omega^*) \approx (0.00024, 14.906)$ , which, as shown in Gallaire and Chomaz,<sup>4</sup> joined with an important complex branch of growth rate curve. This branching point can be found by the fourth order approximation.
- (3) The first and second branches of approximations are seen all overshooting the actual growth rate. The approximations are progressively improved as the order goes up. This suggests that the approximation actually gives an upper bound of the real growth rate.
- (4) Notice that the convergence radius is bounded by  $\sigma_{\max}$ , the maximum growth rate in this neighborhood. This is because the function  $\Omega(\sigma)$  encounters an infinite derivative and loses its analyticity at  $\sigma_{\max}$ . Our computation, however, strongly indicates that the convergence radius is actually  $\sigma_{\max}$ .

We now examine the third and fourth branches of approximations. The results are plotted in Fig. 2. We find the following from this plot.

- (1) The fourth branch of the approximation is similar to the first and second branches. It is again seen that the approximations are straightforward and the obtained value generally overshoots the actual growth rate. A similar branching point  $(\sigma^*, \Omega^*) \approx (0.0017, 15.8934)$  is as well captured.
- (2) The third branch of the approximation has a slightly different behavior. The approximations to the growth rate are seen not any more straightforward. However, the

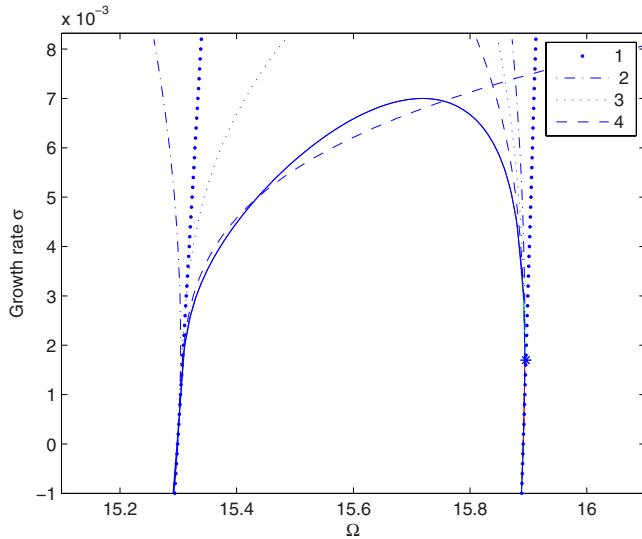


FIG. 2. (Color online) The first to fourth order approximations of the growth rate curves between third and fourth critical swirls. The solid curve indicates the exact solution. The asterisk is the branching point.

obviously more curved growth rate curve is still well approximated in a slightly smaller range of  $\sigma$ .

From this benchmark case study, we may conclude that the growth rate of solid body rotation flow can be effectively found by using the linear operator perturbation method. Theoretically, the growth rate can be completely recovered by the power series. Practically the computational cost for finding the coefficients of this series grows dramatically and only low order approximation shall be used. Our computations have demonstrated that with low order such as fourth order approximation, a significant part of growth rate curve covering  $\sigma$  up to  $\sigma_{\max}/2$  can be found by using the perturbation method.

## V. EXAMPLES: THE LAMB-OSEEN VORTEX AND THE $q$ -VORTEX

In this section, the general method will be applied to the Lamb–Oseen vortex. The computed results will be discussed by comparing them to the case of the solid body rotation flow. Computational issues are also addressed whenever necessary. We then apply the method to the  $q$ -vortex. Both vortices are widely used in the study of vortex breakdown phenomenon.

### A. The Lamb–Oseen vortex with uniform advection

The Lamb–Oseen vortex with uniform advection (here, it will be addressed as the Lamb–Oseen vortex) contains a vortex core at the center in which the flow is similar to the solid body rotation flow, whereas outside this vortex core the flow is close to irrotational flow. The axial velocity of the Lamb–Oseen vortex is uniform and the movement is specified by its axial velocity and its circumferential velocity,

TABLE I. Value of  $\Omega_{1,n}$  for  $n=1,2,3,4$ .

	$n=1$	$n=2$	$n=3$	$n=4$
$\Omega_{1,n}$	0.7824	0.8055	0.8509	0.9171

$$w_0(r) = W_0, \quad (43)$$

$$\omega v_0(r) = \omega \frac{(1 - e^{-r^2/r_c^2})}{r},$$

in which  $\omega$  is the swirl and  $r_c$  is the vortex core. In the study of the stability, the axial velocity can be always rescaled as a unit  $W_0=1$ .

For convenience, let  $\beta=1/r_c^2$ , one finds from Eq. (43)

$$I_0(\psi) = \frac{1 - 2e^{-2\beta\psi} + e^{-4\beta\psi}}{2}, \quad (44)$$

$$I'_0(\psi) = 2\beta e^{-2\beta\psi}(1 - e^{-2\beta\psi}).$$

From Eq. (16), one finds

$$m(y) = \frac{y^2}{\beta(1 - e^{-2\beta y})e^{-2\beta y}}. \quad (45)$$

The stability equation is formulated as the following perturbation problem:

$$\begin{aligned} & \underbrace{-m(y)\left(\phi_{yy} + \frac{\phi_{xx}}{2y}\right)}_{T^{(0)}} + \underbrace{\sigma \int_0^x \left[-2m(y)\left(\phi_{yy} + \frac{\phi_{xx}}{2y}\right)\right] dx}_{T^{(1)}} \\ & + \underbrace{\sigma^2 \int_0^x \int_0^x \left[-m(y)\left(\phi_{yy} + \frac{\phi_{xx}}{2y}\right)\right] dx dx}_{T^{(2)}} = \Omega \phi, \end{aligned} \quad (46)$$

subject to the boundary conditions (18).

The reduced zeroth order eigenvalue problem of  $T^{(0)}$  becomes

$$\Phi_{yy}(y) - \frac{(2n-1)^2 \pi^2 \Phi(y)}{8L^2 y} + \frac{\Omega \beta (1 - e^{-2\beta y}) e^{-2\beta y}}{y^2} \Phi(y) = 0, \quad (47)$$

$$\Phi(0) = 0, \quad \Phi\left(\frac{1}{2}\right) = 0.$$

The ordinary differential equation (47) has been numerically solved by a MATLAB standard solver. For the case  $\beta$  equals 4.0 and  $L$  equals 6.0, one finds the first  $4\Omega_{1,n}$  (see Table I).

In this case, since the axial shear does not present, we shall use Eq. (37) for calculating  $(T^{(1)}\phi_{o1,m}^*, \phi_{o2,n}^*)$  and  $(T^{(2)}\phi_{o1,m}^*, \phi_{o2,n}^*)$ . In the actual evaluation of the above formulas, because of frequent use of the inner products  $(\Phi_{o1,m}^*, \Phi_{o2,n}^*)_1$  and  $(\Phi_{o1,m}^*, \Phi_{o2,n}^*)_3$ , they shall be calculated once only at the beginning of the computation and the result will be recalled promptly.

We are now at a stage to calculate the coefficients  $\Omega_{o,m}^{(i)}$  in the expansion (39). The computation is based on the case  $\beta=4$  and  $L=6$ . We use the explicit formulas of  $(T^{(1)}\phi_{o_1,m}^*, \phi_{o_2,n}^*)$  and  $(T^{(2)}\phi_{o_1,m}^*, \phi_{o_2,n}^*)$  found previously. We found that the summation index  $n=20$  is sufficiently large for obtaining an accurate coefficient. For the summation index  $o$ , our computation demonstrated that the contribution to the growth rate is dominant by  $o=1$  (see Table II for the computation results of  $\Omega_{1,m}^{(2)}$  for the choice of summation index  $o$  up to 1, 2, 3). We find from this table that a choice of summation index up to  $o=3$  is sufficient for obtaining an accurate result.

Table III shows the calculated results of  $\Omega_{1,m}^{(k)}$ . The computation is based on the summation terms up to  $n=20$  and  $o=3$ .

Figure 3 shows the first and second branches of the growth rate curves based on the coefficients shown above. The approximations from the first to the fourth order are similar to what has been found in the case of the solid body rotation flow. We expect that the accuracy of the approximation shall be also similar. In light of the benchmark case study, we may make the following observations for the results obtained.

- (1) The first order approximation is good only in a small  $\sigma$  range, about  $\sigma=0.0005$ , and the second to fourth order approximations extend this range up to  $\sigma=0.0016$ , where the third and fourth order approximations depart from each other. Note that  $\sigma_{\max} < 0.0034$ , where  $\sigma_{\max}$  is the maximum growth rate between the first and second critical swirls.
- (2) The approximation is global in nature. This can be clearly seen from the second branch of approximation. The growth rate has a branching point at  $(\sigma^*, \Omega^*) \approx (0.91 \times 10^{-3}, 0.8057)$  where a complex branch of growth rate curve emanates. This branching point are well captured by the fourth order approximation.
- (3) The approximations are progressively improved as the order goes up in the first and second branch of approximations. It suggests that the approximation overshoots the actual growth rate and thus gives an upper bound of the real growth rate.

To confirm the above statements, we have done numerical simulations of the linearized equations of Eq. (2). Starting from a given but rather arbitrary initial disturbance, the flow eventually evolves into a flow state corresponding to the unstable mode with the largest growth rate. As in this case, only one unstable mode exists and its growth rate can then be found in terms of this long time behavior. The second order

TABLE II. Value of  $\Omega_{1,m}^{(2)}$  calculated with summation index  $o$  up to  $o=1, 2, 3$ .

$o$	$m=1$	$m=2$	$m=3$	$m=4$
1	214.6997	-192.8153	-10.9528	-5.8240
2	214.7012	-192.8136	-10.9516	-5.8218
3	214.7014	-192.8134	-10.9514	-5.8216

TABLE III. Value of  $\Omega_{1,m}^{(k)}$  calculated for  $m=1, 2, 3, 4$  and  $k=1, 2, 3, 4$ .

	$m=1$	$m=2$	$m=3$	$m=4$
$\Omega_{1,m}^{(1)}$	3.8049	0.435 26	0.165 53	0.091 023
$\Omega_{1,m}^{(2)}$	214.70	-192.81	-10.951	-5.8216
$\Omega_{1,m}^{(3)}$	$1.0335 \times 10^5$	$-0.255 13 \times 10^5$	$1.2545 \times 10^3$	$0.969 813 \times 10^2$
$\Omega_{1,m}^{(4)}$	$6.7487 \times 10^6$	$-6.8683 \times 10^6$	$1.0525 \times 10^5$	$-6.4643 \times 10^3$

central difference scheme is used in spatial discretization and the time evolution is integrated by using the fourth order Runge–Kutta method. The simulated growth rates are plotted in Fig. 3 with diamonds. The relation between the actual growth rate and the approximation is indeed very similar to the solid body rotation flow case.

For the computation cost, one notices that the perturbation method is essentially an one-dimensional problem, considering the fact that the axial disturbance has been analytically solved. Significant reduction of computation cost is expected. This has been confirmed by our computations. We have conducted all the computations on same personal computer with Pentium process of 1.5 GHz. The total CPU usage of the perturbation method for finding a fourth order approximation is about 0.16 s, compared to about 1–10 h of CPU usage for computing a single growth rate by direct numerical simulations. We found it difficult to compute the growth rate for  $\Omega$  close to the critical swirl by direct numerical simulations, where the growth rate is in small magnitude; one may have to refine the grids to a sufficient degree to control the truncation error significantly below the growth rate itself. One notices that the perturbation method is most effective at the computation of this range of the swirl.

Figure 4 shows the results of the third and the fourth branches of the growth rate based on the coefficients shown above. We find the following from this plot.

- (1) The fourth branch of the approximation is similar to the

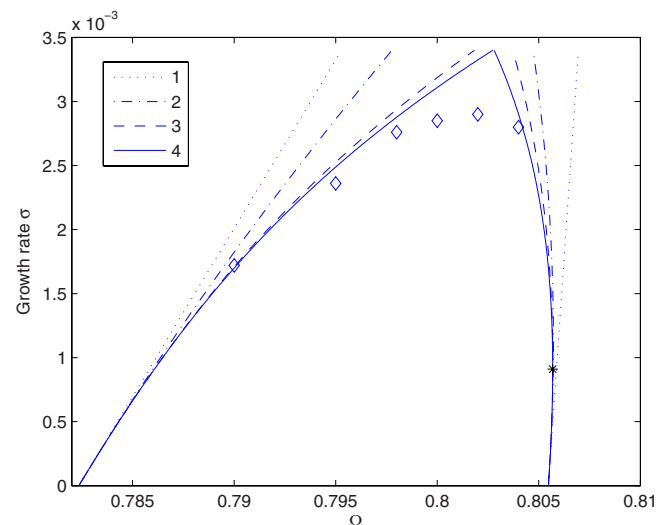


FIG. 3. (Color online) Growth rate  $\sigma$  of the Lamb–Oseen vortex: First and second branches, calculated with first to fourth order approximations. The diamonds are the result of the direct numerical simulations. The asterisk is the branching point.

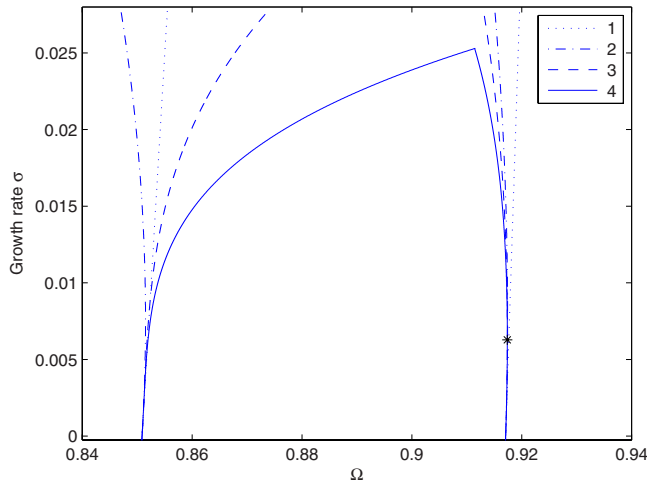


FIG. 4. (Color online) Growth rate  $\sigma$  of the Lamb–Oseen vortex: Third and fourth branches, calculated with first to fourth order approximations. The asterisk is the branching point.

first and second branches. It is again found that the approximation is straightforward. The obtained value is expected to be overshooting the actual growth rate function. A similar branching point  $(\sigma^*, \Omega^*) \approx (0.0063, 0.9174)$  is as well captured.

- (2) The third branch of the approximation is also similar to the solid body rotation case.

Overall, we found that the approximated growth rates are similar to the solid body rotation case. The errors of the

approximations are expected to be of the same magnitude as in the case of the solid body rotation flow.

## B. The $q$ -vortex model

The  $q$ -vortex has a circumferential velocity profile same as the Lamb–Oseen vortex but allows a nonuniform axial velocity distribution,

$$w_0(r) = W_0 + a_0 e^{-r^2}, \quad (48)$$

$$\omega v_0(r) = \omega \frac{(1 - e^{-r^2/r_c^2})}{r},$$

where  $W_0 > 0$  is a constant giving a uniform axial advection and  $a_0$  is a parameter to determine the nature of the axial velocity profile:  $a_0 < 0$  corresponds to a wakelike axial velocity profile and  $a_0 > 0$ , a jetlike.

From Eq. (48), we may derive

$$I_0[\psi_0(y)] = \frac{1 - 2e^{-2\beta y} + e^{-4\beta y}}{2}, \quad (49)$$

$$\{I_0[\psi_0(y)]\}_y = 2\beta e^{-2\beta y}(1 - e^{-2\beta y}),$$

where  $\beta = 1/r_c^2$ . According to Eq. (16), we may find

$$m(y) = \frac{y^2(W_0 + a_0 e^{-r^2})^2}{\beta(1 - e^{-2\beta y})e^{-2\beta y}}. \quad (50)$$

The stability equation of the  $q$ -vortex is found as a perturbation problem,

$$\begin{aligned} & \overbrace{\left[ -m(y) \left( \phi_{yy} + \frac{\phi_{xx}}{2y} - \frac{4a_0 e^{-2y}}{W_0 + a_0 e^{-2y}} \phi \right) \right]}^{T^{(0)}} + \underbrace{\sigma \int_0^x -m(y) \left[ \frac{2}{W_0 + a_0 e^{-2y}} \left( \phi_{yy} + \frac{\phi_{xx}}{2y} \right) - \frac{4a_0 e^{-2y}}{(W_0 + a_0 e^{-2y})^2} \phi \right] dx}_{T^{(1)}} \\ & + \underbrace{\sigma^2 \int_0^x \int_0^x \frac{-m(y)}{(W_0 + a_0 e^{-2y})^2} \left[ \left( \phi_{yy} + \frac{\phi_{xx}}{2y} \right) \right]}_{T^{(2)}} dy = \Omega \phi. \end{aligned} \quad (51)$$

The reduced zeroth order eigenvalue problem of  $T^{(0)}$ , Eq. (51), becomes

$$\begin{aligned} & \Phi_{yy}(y) - \frac{(2n-1)^2 \pi^2 \Phi(y)}{8L^2 y} + \left( \frac{\Omega}{m(y)} - \frac{4a_0 e^{-2y}}{W_0 + a_0 e^{-2y}} \right) \Phi(y) \\ & = 0, \quad \Phi(0) = 0, \quad \Phi(0.5) = 0. \end{aligned} \quad (52)$$

The weighted inner products are found as

$$\begin{aligned} (\Phi_{o_1,m}^*, \Phi_{o_2,n}^*)_1 &= \int_0^{1/2} \frac{\Phi_{o_1,m}^* \Phi_{o_2,n}^*}{m(y)(W_0 + a_0 e^{-2y})} dy, \\ (\Phi_{o_1,m}^*, \Phi_{o_2,n}^*)_2 &= \int_0^{1/2} \frac{4a_0 e^{-2y}}{(W_0 + a_0 e^{-2y})^2} \Phi_{o_1,m}^* \Phi_{o_2,n}^* dy, \\ (\Phi_{o_1,m}^*, \Phi_{o_2,n}^*)_3 &= \int_0^{1/2} \frac{\Phi_{o_1,m}^* \Phi_{o_2,n}^*}{m(y)(W_0 + a_0 e^{-2y})^2} dy, \end{aligned} \quad (53)$$

$$(\Phi_{o_1,m}^*, \Phi_{o_2,n}^*)_4 = \int_0^{1/2} \frac{4a_0 e^{-2y}}{(W_0 + a_0 e^{-2y})^3} \Phi_{o_1,m}^* \Phi_{o_2,n}^* dy.$$

These are explicit formulas used in the computation of the perturbation method. For the cases  $\beta=4$ ,  $W_0=1$ ,  $a_0=\pm 0.2$ , and  $L=6$ , we find the fourth order approximations, and the results are plotted in Figs. 5(a) and 5(b).

## VI. SWIRLING FLOW WITH FIXED FLOWRATE AT THE OUTLET

We address the stability problem with changing the outlet boundary condition to

$$\phi(t, L) = 0, \quad (54)$$

which corresponds to the physical setting: A fixed flowrate at the discharge. We consider two types of vortices: Solid body rotation flow as a benchmark case and the Lamb–Oseen vortex. The results obtained are important for the study of the physical mechanism of the swirling flow in a finite pipe. It can be shown that the energy transfer mechanism of this boundary setting is simpler than the boundary condition (8).

$$I_1(m, n) = \begin{cases} \frac{4L}{m^2 \pi^2} (1 - (-1)^n) & \text{if } n = m, \\ \frac{4L}{m \pi^2} \left[ \frac{1 - (-1)^n}{n} + \frac{(-1)^{(n+m)} - 1}{2(n+m)} + \frac{(-1)^{(n-m)} - 1}{2(n-m)} \right] & \text{if } n \neq m, \end{cases} \quad (58)$$

and

$$I_2(m, n) = \begin{cases} -\frac{L^2}{m^2 \pi^2} \left[ 1 + (-1)^n \frac{2}{\pi} \right] & \text{if } n = m, \\ (-1)^{n+1} \frac{2L^2}{mn \pi^3} & \text{if } n \neq m. \end{cases} \quad (59)$$

One thus obtains

$$\begin{aligned} (T^{(1)} \phi_{o_1,m}^*, \phi_{o_2,n}^*) &= I_1(m, n) \left[ \Omega_{o_1,m}(\Phi_{o_1,m}^*, \Phi_{o_2,n}^*)_1 \right. \\ &\quad \left. - \frac{1}{2}(\Phi_{o_1,m}^*, \Phi_{o_2,n}^*)_2 \right], \\ (T^{(2)} \phi_{o_1,m}^*, \phi_{o_2,n}^*) &= I_2(m, n) \left[ \Omega_{o_1,m}(\Phi_{o_1,m}^*, \Phi_{o_2,n}^*)_3 \right. \\ &\quad \left. - (\Phi_{o_1,m}^*, \Phi_{o_2,n}^*)_4 \right]. \end{aligned} \quad (60)$$

A noticeable fact is  $I_1(m, m)=0$  for  $m$  even, and thus  $\Omega_{o,m}^{(1)}=0$ .

## A. General approach

The general method introduced in Sec. II can be modified to treat this type of boundary conditions. We follow all the steps up to Eq. (24) and change Eq. (25) to

$$\phi_{o,n}^*(x, y) = \sqrt{\frac{2}{L}} \Phi_{o,n}^*(y) \sin\left(\frac{n\pi x}{L}\right), \quad (55)$$

with  $\Phi_{o,n}^*(y)$  solving the reduced zeroth order eigenvalue problem

$$\Phi_{yy}(y) - \frac{n^2 \pi^2 \Phi(y)}{2L^2 y} + \left[ \frac{\Omega_{o,n}}{m(y)} - \frac{w_{0yy}}{w_0} \right] \Phi(y) = 0, \quad (56)$$

$$\Phi(0) = 0, \quad \Phi\left(\frac{1}{2}\right) = 0,$$

and normalized according to Eq. (27). This change is due to the fact that the  $x$ -direction eigenfunction  $\sin[(2n-1)\pi x/2L]$  is now replaced by  $\sin(n\pi x/L)$ ,

We then derive explicit expressions of

$$(T^{(1)} \phi_{o_1,m}^*, \phi_{o_2,n}^*) \quad \text{and} \quad (T^{(2)} \phi_{o_1,m}^*, \phi_{o_2,n}^*) \quad (57)$$

in terms of the eigenfunctions (55). In a similar manner, the following functions can be derived to replace Eqs. (32) and (33):

## B. Examples

We apply the method to the solid body rotation flow with pipe length  $L=10$ . The first to fourth order approximations and the comparison to the exact growth rate are plotted in Figs. 6(a) and 6(b). We find from this plot that the overall behavior of the approximations is very similar to the case with boundary conditions (8).

We also apply the method to the Lamb–Oseen vortex with the case  $\beta=4$  and  $L=6$ . The first to fourth order approximations are plotted in Figs. 7(a) and 7(b). The growth rate curve again resembles to the solid body rotation flow.

## VII. COMPLEX GROWTH RATE BRANCH

It has been found in Gallaire and Chomaz<sup>4</sup> and Gallaire and Chomaz and Huerre<sup>10</sup> that, besides the real growth rate branch, there exist complex growth rate branches for the solid body rotation flow. The complex growth rates are found to be complex conjugates. The modes associated with the complex growth rate are unstable and oscillating. One would expect that similar complex branches should exist for general columnar swirling flows.

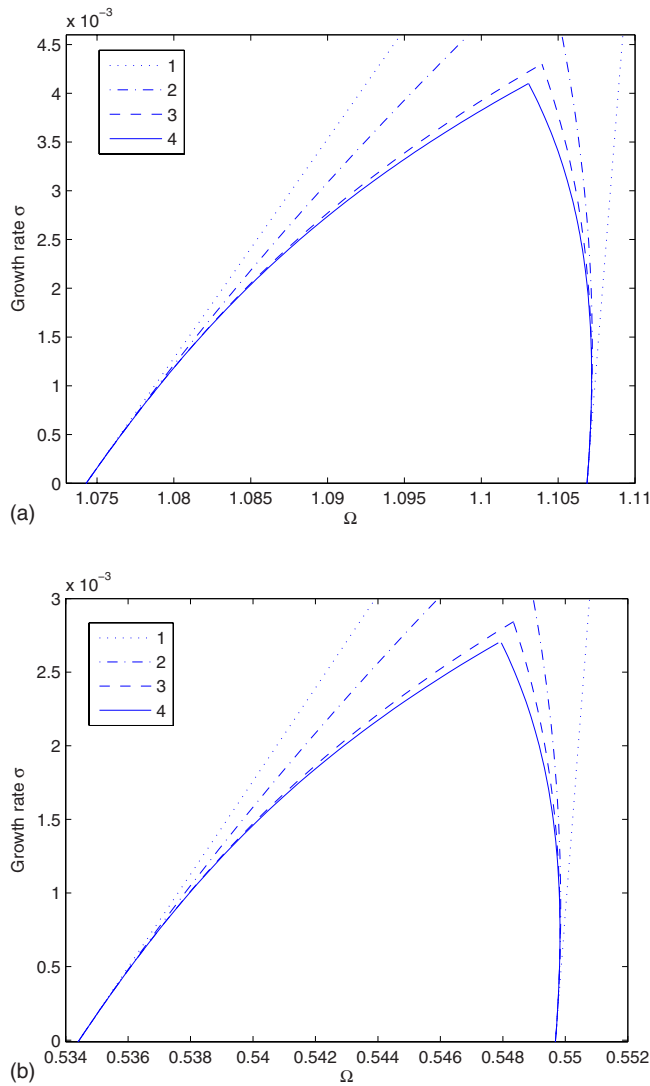


FIG. 5. (Color online) First and second branches of growth rate  $\sigma$  of the  $q$ -vortex, calculated with first to fourth order approximations. (a)  $W_0=1$  and  $a_0=0.2$ ; (b)  $W_0=1$  and  $a_0=-0.2$ .

The perturbation method discussed here is a global method, in the sense that the analyticity of the function  $\Omega(\sigma)$  is an established fact and the power series obtained by the perturbation method is convergent in the complex plane up to the nearest nonanalytic point. Although it has not been mathematically proved that the convergence radius is exactly equal to  $\sigma_{\max}$ , all computational results indicate that this is the case. In the following, we will make use of this analyticity and extend the relation between  $\Omega$  and  $\sigma$  to the complex domain. The analytic continuation of the approximated polynomial will lead to the complex growth rate branch.

We first consider the case of the solid body rotation flow with the fixed flowrate at the outlet. We found the second branch of approximation as

$$\Delta_{1,2}\Omega(\sigma) \approx -2.1356 \times 10^4 \sigma^2 - 9.6514 \times 10^6 \sigma^3 - 5.3268 \times 10^9 \sigma^4, \quad (61)$$

and the coefficient of  $\sigma$  vanishes and all the other coefficients are negative. Therefore, the swirl increment  $\Delta_{1,2}\Omega$  is always negative for real  $\sigma$ . However, if we extend the func-

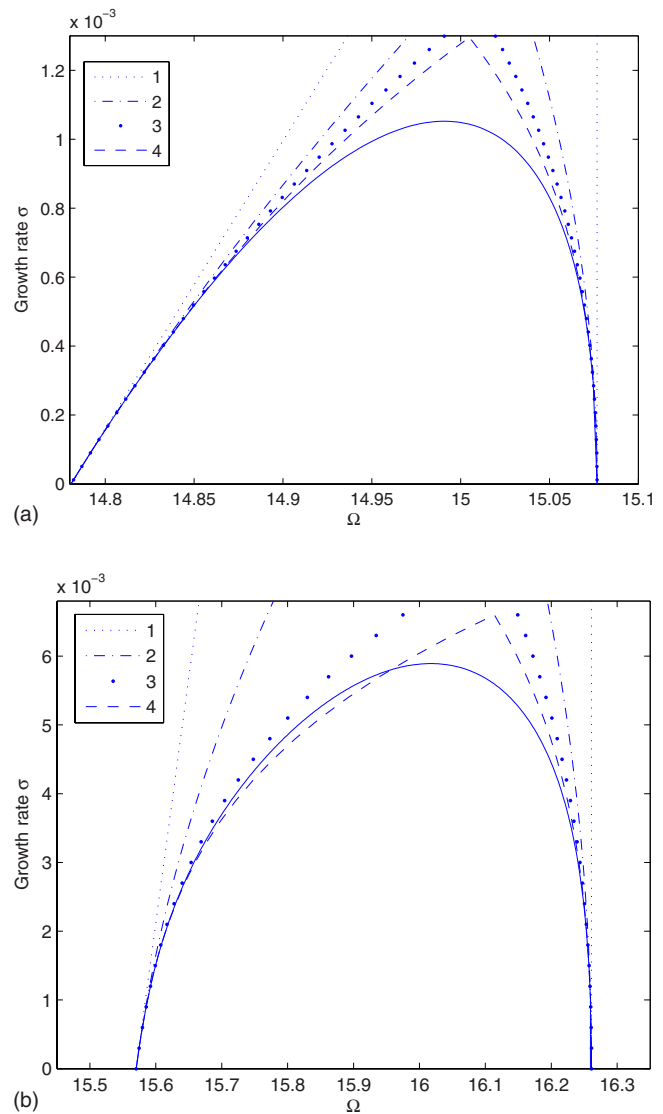


FIG. 6. (Color online) Growth rate  $\sigma$  of the solid body rotation flow with fixed outlet flow, calculated with first to fourth order approximations. (a) First and second branches; (b) third and fourth branches. The solid curves indicate the exact solutions.

tion  $\Delta_{1,2}\Omega(\sigma)$  to the complex plane, we may find a complex growth rate  $\sigma$ , which gives rise a positive swirl increment  $\Delta_{1,2}\Omega(\sigma) > 0$ . The growth rate function can be extended to the swirl above the critical swirl  $\Omega_{1,2}$ .

To proceed, we need only to seek a complex  $\sigma$  to solve Eq. (61) for a given  $\Omega > \Omega_{1,2}$ . The result is shown in Figs. 8(a) and 8(b). The exact growth rate function is plotted in this figure for comparison. It is found that the complex branch is well approximated in this neighborhood.

Notice that the approximation worsens as the norm of the complex growth rate  $\sigma$  is close to  $\sigma_{\max}$  (where  $\Omega \approx 15.1$ ). This again indicates that the actual convergence radius of the power series is  $\sigma_{\max}$ .

Applying this method to the Lamb–Oseen vortex with the same boundary conditions generates the complex branch for  $\Omega > \Omega_{1,2}$ . This complex branch is shown in Fig. 9. It is found from this plot that the curve of the imaginary part of the complex growth rate rises considerably slower than for

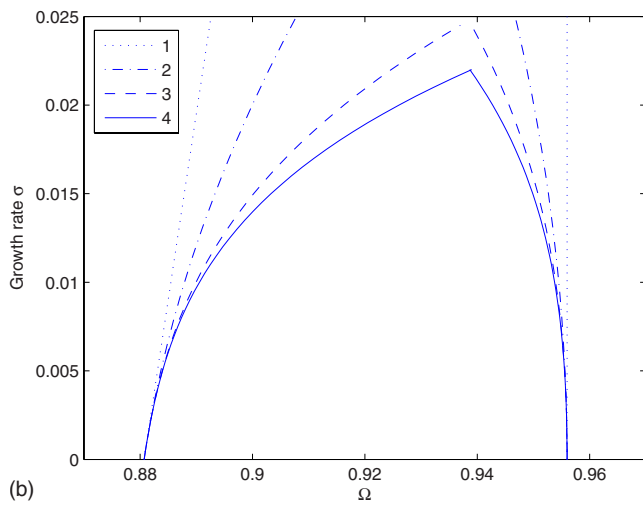
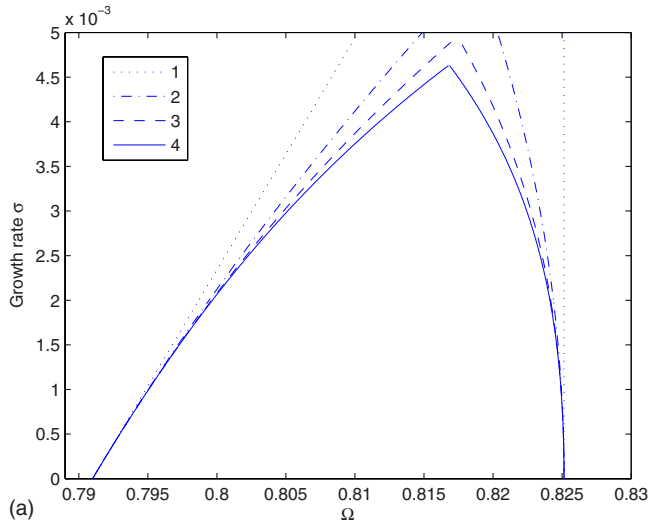


FIG. 7. (Color online) Growth rate  $\sigma$  of the Lamb–Oseen vortex with fixed outlet flow, calculated with first to fourth order approximations. (a) First and second branches; (b) third and fourth branches.

the case of the solid body rotation flow, and the norm of the growth rate  $\sigma$  reaches the level of  $\sigma_{\max}$  at swirl level approximately  $\Omega=0.828$ . The approximation of the complex branch is expected to be good up to  $\Omega=0.828$ .

### VIII. THE STUDY OF THE ENERGY TRANSFER MECHANISM OF THE LAMB–OSEN VORTEX

We consider an application of the current method: The energy transfer mechanism of the Lamb–Oseen vortex in a finite pipe. It has been shown in Gallaire and Chomaz<sup>4</sup> that the stability of the solid body rotation flow is solely dependent on the net gain of the energy at the inlet and outlet. The internal flow is inactive in the energy transfer between the disturbance and the base flow. Is this generally true for vortex flows in a finite pipe? We will show by using the current method that the answer to this question is negative: The solid body rotation is but an exceptional case, and, in general, the internal flow is active in energy transfer.

The kinetic energy of the disturbance contained in a finite pipe is (with multiplying density)

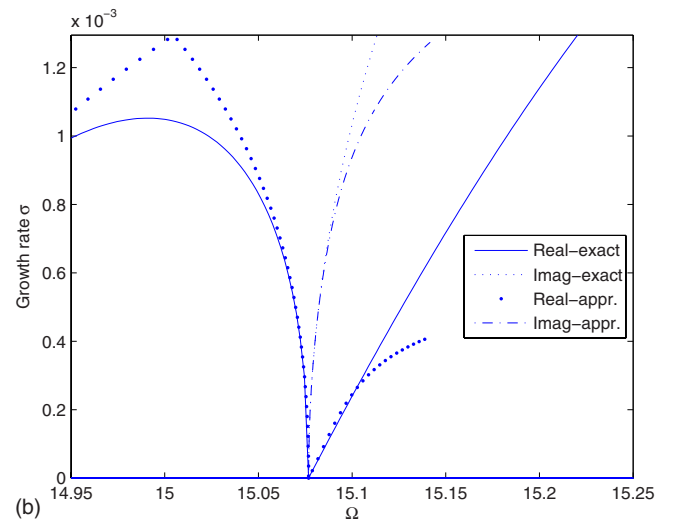
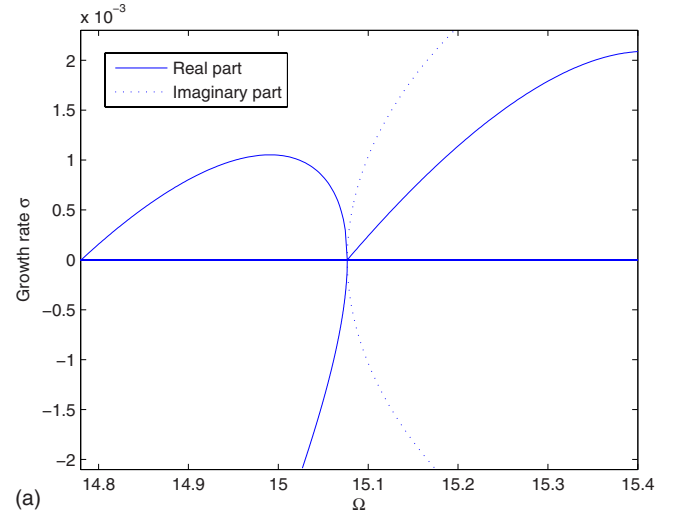


FIG. 8. (Color online) Complex growth rate  $\sigma$  of the solid body rotation flow with fixed outlet flow. (a) The exact growth rate; (b) the comparison to the fourth order approximation.

$$E(t) = 2\pi \int_D \frac{1}{2}(u_1^2 + v_1^2 + w_1^2) dy dx, \quad (62)$$

where  $u_1$ ,  $v_1$ , and  $w_1$  are radial, azimuthal, and axial velocities of the disturbance, respectively. For an axisymmetric base flow with velocity components  $(U, V, W)$ , one has the following Reynolds–Orr equation (see Schmid and Henningson<sup>11</sup> and Wu *et al.*<sup>12</sup>):

$$\begin{aligned} \frac{dE(t)}{dt} = 2\pi \left( \int_D -(u_1, v_1, w_1) \mathbf{B}(u_1, v_1, w_1)^T dx dy \right. \\ \left. - \int_0^{0.5} [u_1 p_1]_{x=0}^{x=L} dy \right. \\ \left. - \frac{1}{2} \int_0^{0.5} [W(u_1^2 + v_1^2 + w_1^2)]_{x=0}^{x=L} dy \right), \quad (63) \end{aligned}$$

where  $p_1$  is the disturbance of the pressure and  $\mathbf{B}$  is the symmetric strain rate of the base flow,

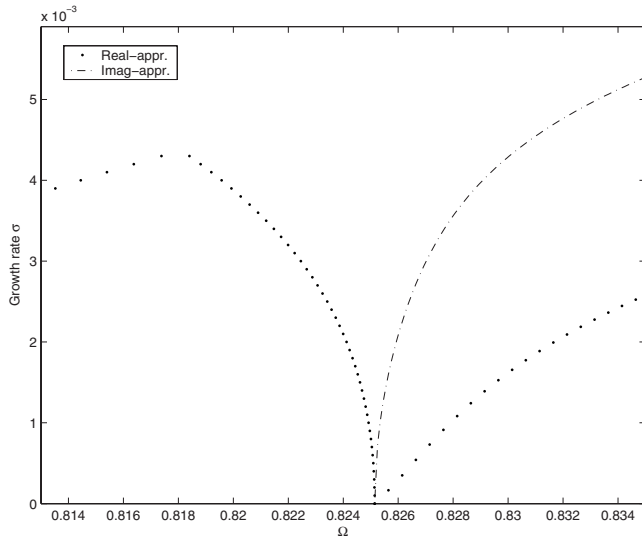


FIG. 9. Fourth order approximation of the complex growth rate  $\sigma$  of the Lamb–Oseen vortex with fixed outlet flow.

$$\mathbf{B} = \frac{1}{2} \begin{bmatrix} 2U_r & r\left(\frac{V}{r}\right)_r & W_r + U_x \\ r\left(\frac{V}{r}\right)_r & \frac{2U}{r} & V_x \\ W_r + U_x & V_x & 2W_x \end{bmatrix}. \quad (64)$$

For the columnar swirling flow with uniform axial flow  $W \equiv 1$ , one obtains from Eqs. (63) and (64)

$$\begin{aligned} \frac{dE(t)}{dt} = 2\pi & \left( - \int_D \omega \left( \frac{dv_0}{dr} - \frac{v_0}{r} \right) v_1 u_1 dy dx \right. \\ & - \int_0^{0.5} [w_1 p_1]_{x=0}^{x=L} dy \\ & \left. - \frac{1}{2} \int_0^{0.5} [u_1^2 + v_1^2 + w_1^2]_{x=0}^{x=L} dy \right). \end{aligned} \quad (65)$$

The first term in right hand side (RHS) represents the contribution to the kinetic energy of the disturbance from the internal flow. The second term in RHS represents the work done to the disturbance due to the pressure disturbance, which is exerted on the fluid at the inlet and outlet. The third term in RHS represents the disturbance's kinetic energy flux at the inlet and outlet.

One notices that for the solid body rotation flow, the term  $(dv_0/dr - v_0/r)$  vanishes in the entire flow field, and thus the kinetic energy transfer cannot take place in the flow. This recovers Gallaire and Chomaz's result in a straightforward manner. For other vortex flow the same term cannot be vanished over the entire flow field, and the internal energy transfer presumably takes place.

We consider the Lamb–Oseen vortex with the fixed flowrate boundary condition imposed at the outlet, Eq. (54), as a representation case study. The growth rate function has been calculated in Sec. VI for the case  $\beta=4$  and  $L=6$ . The

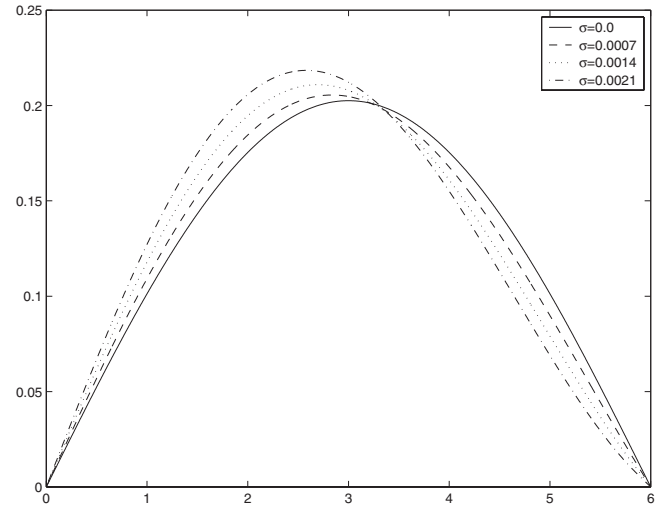


FIG. 10. The eigenfunctions  $\phi(x, y; \sigma)$  for  $\sigma=0, 0.0007, 0.0014, 0.0021$  and  $y=0.1$ .

fixed flowrate boundary condition has an advantage that the second term in Eq. (65) becomes inactive. For the Lamb–Oseen vortex, one finds

$$\frac{dv_0}{dr} - \frac{v_0}{r} = 2\beta e^{-2\beta y} - \frac{(1 - e^{-2\beta y})}{y}. \quad (66)$$

The Reynolds–Orr equation therefore reads as

$$\begin{aligned} \frac{dE(t)}{dt} = 2\pi & \left\{ \int_0^{0.5} \int_0^L -\omega \left[ 2\beta e^{-2\beta y} \right. \right. \\ & \left. \left. - \frac{(1 - e^{-2\beta y})}{y} \right] u_1 v_1 dx dy \right. \\ & \left. + \frac{1}{2} \int_0^{0.5} [u_1^2 + v_1^2]_{x=0}^{x=L} dy \right\}. \end{aligned} \quad (67)$$

To proceed further, the flow field of the disturbance,  $u_1$  and  $v_1$ , must be found. This task can be done by using the perturbation method, as described in Appendix A 3. Consider the first branch of the growth rate function of the Lamb–Oseen vortex with  $\beta=4$  and  $L=6$ , which is calculated in Sec. VI and plotted in Fig. 7(a). One finds that the critical swirl  $\Omega_{1,1} \approx 0.791$ . Above  $\Omega_{1,1}$  the flow becomes unstable. As shown in Fig. 7(a), the second order approximation of the growth rate function is valid for  $\sigma$  up to 0.0025. The corresponding eigenfunctions  $\phi(x, y; \sigma)$  for  $\sigma = 0, 0.0007, 0.0014, 0.0021$ , with second order accuracy, are found, and a typical slice of this function,  $\phi(x, 0.1; \sigma)$ , is plotted in Fig. 10. A noticeable feature of the eigenfunctions is that they become more asymmetric as  $\sigma$  increases. The asymmetry reflects the influence of the boundary.

Notice that in the linear growth range,  $u_1$  and  $v_1$  are exponential functions of  $t$  and can be written as  $u_1(x, y, t) = \epsilon \bar{u}_1(x, y) e^{\sigma t}$  and  $v_1(x, y, t) = \epsilon \bar{v}_1(x, y) e^{\sigma t}$ , respectively.  $\bar{u}_1(x, y)$  and  $\bar{v}_1(x, y)$  can be directly found from  $\phi(x, y)$ . One may write Eq. (67) in terms of  $\bar{u}_1(x, y)$  and  $\bar{v}_1(x, y)$  as

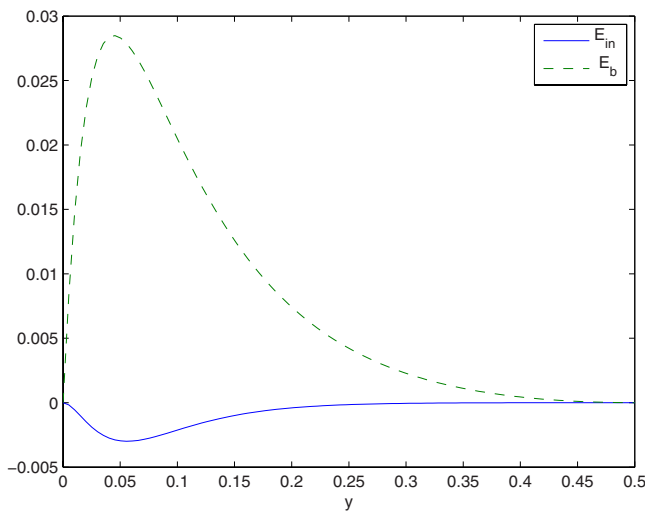


FIG. 11. (Color online) The density functions of the energy transfer rate:  $E_{in}(y; \sigma)$  and  $E_b(y; \sigma)$  for  $\sigma=0.001$ . It is shown that the magnitude of  $E_{in}(y; \sigma)$  is much smaller than  $E_b(y; \sigma)$ , and  $E_{in}(y; \sigma) < 0$ .

$$\frac{dE(t)}{dt} = 2\pi\epsilon^2 e^{2\sigma t} \int_0^{0.5} [E_{in}(y; \sigma) + E_b(y; \sigma)] dy + o(\epsilon^2), \quad (68)$$

where

$$E_{in}(y; \sigma) = -\omega \left[ 2\beta e^{-2\beta y} - \frac{(1 - e^{-2\beta y})}{y} \right] \int_0^L \bar{u}_1 \bar{v}_1 dx \quad (69)$$

and

$$E_b(y; \sigma) = \frac{1}{2} [\bar{u}_1^2 + \bar{v}_1^2]_{x=0}^{x=L}. \quad (70)$$

$E_b(y; \sigma)$  represents the density of the boundary energy transfer rate at the radial location  $y$ , and  $E_{in}(y; \sigma)$  the density of the internal energy transfer rate at  $y$ , which takes into account of the axially accumulated effect. Equation (68) separates the roles of the internal flow and the boundary.

One proceeds to calculate  $E_{in}(y; \sigma)$  and  $E_b(y; \sigma)$  from Eqs. (69) and (70). The results are plotted in Fig. 11. It is evident from this plot that the energy transfer between the base flow and the disturbance does take place in the internal flow. It was found that the internal energy transfer in this case is less than 10% of the total energy transfer, and the majority of the energy exchange still occurs at the boundaries. This gives a good explanation why the growth rate curve of the Lamb–Oseen vortex resembles the solid body rotation flow. Moreover, the sign of  $E_{in}$  is negative, which indicates that the kinetic energy is transferred from the disturbance to the base flow in the internal flow. The instability is still generated by the energy gain of the disturbance at the boundaries. It shall be remarked that for the Lamb–Oseen vortex in an infinite pipe, there is no net energy transfer in the internal flow. However, for swirling flows in finite pipe, the presence of the physical boundaries has an influence over the entire flow field and may induce the internal energy transfer.

In this study of the physical mechanism, the perturbation method has shown its strength. The estimated energy transfer rates, obtained by the perturbation method, are accurate in second order for swirl sufficiently close to the critical swirl. This makes the conclusion thus drawn stand on a more solid ground. One notices that the magnitude of the growth rate and the degree of the asymmetry of the mode shape are small in the range of interest. The perturbation method certainly has an advantage over the numerical method in this range of swirl.

## IX. CLOSING REMARKS

We develop a new method based on the perturbation method of linear operators to solve the global stability problem for columnar inviscid swirling flows in a finite pipe. The method has the following advantages.

- (1) The method works for all columnar swirling flows in a finite pipe.
- (2) The method is of a semianalytic nature in the sense that all the analyses, in terms of the axial disturbance, have been analytically resolved. This effectively reduces the dimension of the problem by one. The computation cost of the direct numerical computation of the stability problem (17), as an eigenvalue problem of two dimensions, is much more expensive.
- (3) It provides an algebraic form for the growth rate function and an analytic representation for the eigenmode. This is particularly useful in the study of the physical mechanism.

This method fills a technical gap in the study of the dynamics of the swirling flows in a finite pipe. Previously, only for one single flow, the solid body rotation flow, the global stability has been analyzed. As such, the research scope was unavoidably confined to this particular flow configuration. Now, more realistic vortex flows, such as the Lamb–Oseen vortex and  $q$ -vortex can all be analyzed by this method. We have applied the method to the Lamb–Oseen vortex and  $q$ -vortex and found their growth rate functions for two types of boundary conditions. This reveals their general stability behaviors and opens doors for further investigations of the dynamical behaviors under various flow conditions. As an application, we use the method to study the energy transfer mechanism of the Lamb–Oseen vortex in a finite pipe and reveal a rather striking physical fact that the internal flow is actively engaged in the energy transfer between the disturbance and the base flow due to the influence of the boundaries. As has been shown, the analytic form of the eigenmode found by the current method is, indeed, useful in this application. We anticipate that the method can be effectively applied to many other flow problems.

## ACKNOWLEDGMENTS

This research was carried out with the support of Auckland University under Grant No. 3606871/9344.

## APPENDIX A: THE PERTURBATION METHOD

We introduce the perturbation method of the linear operators in this section. We do not intend to cover the general perturbation method, which could become very complicated technically. We recommend Kato<sup>13</sup> for further reading, which is our general reference. In the following, we introduce the basic formulas in the perturbation method, and we restrict our attention to the case where the unperturbed operator  $T^{(0)}$  is a self-adjoint operator and the spectrum of  $T^{(0)}$  is discrete and simple. This makes the description of the method much more concisely, yet being sufficient for the application in the stability problem.

### 1. The basic formulas in perturbation method

Consider the linear operator  $T(\sigma)$  with the form

$$T(\sigma) = T^{(0)} + \sigma T^{(1)} + \sigma^2 T^{(2)}, \quad (\text{A1})$$

in which  $T^{(0)}$  is assumed as an unbounded self-adjoint linear operator with a densely defined domain in a Hilbert space  $\mathbf{H}$  and  $T^{(1)}$  and  $T^{(2)}$  are assumed linear operators relatively bounded by  $T^{(0)}$ , that is, there exist constants  $a$  and  $b$  such that

$$\max(\|T^{(1)}u\|, \|T^{(2)}u\|) \leq a\|u\| + b\|T^{(0)}u\| \quad (\text{A2})$$

on the domain. Under these assumption,  $T(\sigma)$  is proved in Kato,<sup>13</sup> a homomorphic function of  $\sigma$ .

Furthermore, we assume that the spectrum of  $T^{(0)}$  is discrete and simple, denoted by  $\lambda_0, \lambda_1, \lambda_2, \dots$ , with the corresponding orthonormal eigenvectors  $\{e_0, e_1, e_2, \dots\}$  (the eigenvalues are aptly denoted by  $\lambda$  rather than the swirl parameter  $\Omega$  for avoiding possible confusion),

$$\begin{aligned} T^{(0)}e_0 &= \lambda_0 e_0, \\ T^{(0)}e_i &= \lambda_i e_i, \quad i = 1, 2, \dots \end{aligned} \quad (\text{A3})$$

We single out the eigenvalue  $\lambda_0$  here with which we are going to consider the perturbation problem: How does this eigenvalue change if the perturbed term  $\sigma T^{(1)} + \sigma^2 T^{(2)}$  is present? We shall denote the perturbed eigenvalue as  $\lambda(\sigma)$  to indicate the dependence. From the perturbation theory, we know that, in general, the eigenvalue  $\lambda(\sigma)$  is an analytic function of  $\sigma$  in a neighborhood of  $\sigma=0$ , and thus  $\lambda(\sigma)$  admits a power series expansion in the neighborhood,

$$\lambda(\sigma) = \lambda_0 + \sum_{n=1}^{\infty} \lambda^{(n)} \sigma^n. \quad (\text{A4})$$

The coefficients  $\lambda^{(n)}$  can be found from the operators  $T^{(0)}$ ,  $T^{(1)}$ , and  $T^{(2)}$  and the convergence radius can be proved to be always positive.

Before introducing the formulas with which we can calculate  $\lambda^{(n)}$ , we need to define some relevant operators that are derived from the unperturbed operator  $T^{(0)}$ . For the eigenvalue  $\lambda_0$  and the eigenspace  $\{e_0\}$ , consider the following operators.

- (1) The projection  $P$  onto the subspace spanned by  $e_0$ ,

$$Pu = (u, e_0)e_0. \quad (\text{A5})$$

- (2) The reduced resolvent  $S$  which can be expressed in terms of the basis  $\{e_0, e_1, e_2, \dots\}$  as

$$Su = \sum_{i=1}^{\infty} (\lambda_i - \lambda_0)^{-1} (u, e_i) e_i. \quad (\text{A6})$$

$S$  can be thought as an inverse of  $T^{(0)} - \lambda_0 I$  on the orthogonal complement of the eigenspace  $\{e_0\}$ . Indeed, we can make this a little more specific. Let  $\tilde{T}^{(0)}$  and  $\tilde{S}$  be the restrictions of operators  $T^{(0)}$  and  $S$  to the invariant subspace  $(I - P_0)\mathbf{H}$  (i.e., the orthogonal complement of the eigenspace  $\{e_0\}$ ), respectively, then

$$\tilde{S} = (\tilde{T}^{(0)} - \lambda I)^{-1}. \quad (\text{A7})$$

It is interesting to observe that  $P$  and  $S$  completely represent  $T^{(0)}$  in the perturbation method. The advantage of this representation is that  $P$  and  $S$  have simple expressions in terms of the basis. The contributions to the perturbed eigenvalue are then determined by the mutual interactions between  $P$ ,  $S$ ,  $T^{(1)}$ , and  $T^{(2)}$ , and a formula has been neatly derived (see, for example, Kato<sup>13</sup>) to represent such interactions and to enable us to calculate the coefficients  $\lambda^{(n)}$  in the expansion,

$$\begin{aligned} \lambda^{(n)} &= \sum_{p=1}^n \frac{(-1)^p}{p} \\ &\times \sum_{v_1 + \dots + v_p = n, k_1 + \dots + k_p = p-1} \text{tr}[T^{(v_1)} S^{(k_1)} \dots T^{(v_p)} S^{(k_p)}], \end{aligned} \quad (\text{A8})$$

where  $S^{(k)} = S^k$  for integer  $k > 0$ ,  $S^{(0)} = -P$ , and the symbol  $\text{tr}$  stands for the trace of a linear operator, which can be defined for any operator with finite rank, as is the case here. Notice that in this formula, the sum should be taken over all combinations of positive integers  $p$  with  $1 \leq p \leq n$  and  $v_1, v_2, \dots, v_p$  with  $v_j = 1$  or  $2$ ,  $v_1 + \dots + v_p = n$  and  $k_1 + \dots + k_p = p - 1$ . Although Eq. (A8) appears complicated, it is nevertheless the most efficient way to represent  $\lambda^{(n)}$ . Besides, a procedure can be developed to write up all the terms in Eq. (A8) and this is done in the next section.

### 2. The derivation of the formulas used in perturbation method

In Kato,<sup>13</sup> the terms in Eq. (A8) up to  $\lambda^{(4)}$  have been explicitly given as

$$\begin{aligned}
\lambda^{(1)} &= \text{tr}[T^{(1)}P], \\
\lambda^{(2)} &= \text{tr}[T^{(2)}P - T^{(1)}ST^{(1)}P], \\
\lambda^{(3)} &= \text{tr}[-T^{(1)}ST^{(2)}P - T^{(2)}ST^{(1)}P + T^{(1)}ST^{(1)}ST^{(1)}P - T^{(1)}S^2T^{(1)}PT^{(1)}P], \\
\lambda^{(4)} &= \text{tr}[-T^{(2)}ST^{(2)}P + T^{(1)}ST^{(1)}ST^{(2)}P + T^{(1)}ST^{(2)}ST^{(1)}P + T^{(2)}ST^{(1)}ST^{(1)}P - T^{(1)}S^2T^{(1)}PT^{(2)}P - T^{(1)}S^2T^{(2)}PT^{(1)}P \\
&\quad - T^{(2)}S^2T^{(1)}PT^{(1)}P - T^{(1)}ST^{(1)}ST^{(1)}ST^{(1)}P + T^{(1)}S^2T^{(1)}ST^{(1)}PT^{(1)}P + T^{(1)}ST^{(1)}S^2T^{(1)}PT^{(1)}P + T^{(1)}S^2T^{(1)}PT^{(1)}ST^{(1)}P \\
&\quad - T^{(1)}S^3T^{(1)}PT^{(1)}PT^{(1)}P].
\end{aligned} \tag{A9}$$

These formulas are essential in the perturbation method. One may find similar formulas for high order  $\lambda^{(n)}$ .

The next step is to evaluate the trace of the operators in the formulas obtained. This can be carried out with the following formula:

$$\text{tr} AP = (APe_0, e_0) = (Ae_0, e_0), \tag{A10}$$

which is valid for any linear operator  $A$ . Applying Eqs. (A10) and (A9), one obtains

$$\lambda^{(1)} = (T^{(1)}e_0, e_0). \tag{A11}$$

By using the explicit expression of the operator  $S$ , Eq. (A7), whenever applicable, one obtains

$$\begin{aligned}
\lambda^{(2)} &= (T^{(2)}e_0, e_0) - (T^{(1)}ST^{(1)}e_0, e_0) \\
&= (T^{(2)}e_0, e_0) - \sum_i \frac{(T^{(1)}e_0, e_i)(T^{(1)}e_i, e_0)}{(\lambda_i - \lambda_0)},
\end{aligned} \tag{A12}$$

where  $\sum_i = \sum_{i=1}^{\infty}$  and in all the following, we adopt the same notation. It is found that all other  $\lambda^{(n)}$  can be derived in a similar way.  $\lambda^{(3)}$  appears as

$$\begin{aligned}
\lambda^{(3)} &= - \sum_i \frac{(T^{(2)}e_0, e_i)(T^{(1)}e_i, e_0)}{(\lambda_i - \lambda_0)} \\
&\quad - \sum_i \frac{(T^{(1)}e_0, e_i)(T^{(2)}e_i, e_0)}{(\lambda_i - \lambda_0)} \\
&\quad + \sum_{i,j} \frac{(T^{(1)}e_0, e_i)(T^{(1)}e_i, e_j)(T^{(1)}e_j, e_0)}{(\lambda_i - \lambda_0)(\lambda_j - \lambda_0)} \\
&\quad - \sum_i \frac{(T^{(1)}e_0, e_0)(T^{(1)}e_0, e_i)(T^{(1)}e_i, e_0)}{(\lambda_i - \lambda_0)^2}.
\end{aligned} \tag{A13}$$

One may easily find a similar but much lengthy formula for  $\lambda^{(4)}$  from Eq. (A9).

### 3. Find the eigenmodes from the projection

Let  $\mathbf{P}(\sigma)$  be the projection onto the eigenspace of  $T(\sigma)$  for the perturbed eigenvalue  $\lambda(\sigma)$ . One has the following expansion for  $\mathbf{P}(\sigma)$ :

$$\mathbf{P}(\sigma) = P + \sigma P^{(1)} + \sigma^2 P^{(2)} + \dots, \tag{A14}$$

where  $P$  is the same project operator as appeared in the expansion of Eq. (A9) and  $P = \mathbf{P}(0)$ , and

$$\begin{aligned}
P^{(1)} &= -PT^{(1)}S - ST^{(1)}P, \\
P^{(2)} &= -PT^{(2)}S - ST^{(2)}P + PT^{(1)}ST^{(1)}S + ST^{(1)}PT^{(1)}S \\
&\quad + ST^{(1)}ST^{(1)}P - PT^{(1)}PT^{(1)}S^2, \\
&\quad - PT^{(1)}S^2T^{(1)}P - S^2T^{(1)}PT^{(1)}P.
\end{aligned} \tag{A15}$$

By using Eq. (A14), one may find the eigenvector of  $T(\sigma)$  in the second order accuracy as

$$\mathbf{P}(\sigma)e_0 = e_0 + \sigma P^{(1)}e_0 + \sigma^2 P^{(2)}e_0, \tag{A16}$$

where  $e_0$  is the eigenfunction of the unperturbed operator  $T(0)$ .

Noticing  $Pe_0 = e_0$  and  $Se_0 = 0$ , one obtains

$$\begin{aligned}
P^{(1)}e_0 &= -ST^{(1)}e_0, \\
P^{(2)}e_0 &= -ST^{(2)}e_0 + ST^{(1)}ST^{(1)}e_0 - PT^{(1)}S^2T^{(1)}e_0 \\
&\quad - S^2T^{(1)}PT^{(1)}e_0.
\end{aligned} \tag{A17}$$

By using Eqs. (A5) and (A6), one derives from Eq. (A17)

$$P^{(1)}e_0 = - \sum_i \frac{(T^{(1)}e_0, e_i)e_i}{(\lambda_i - \lambda_0)} \tag{A18}$$

and

$$\begin{aligned}
P^{(2)}e_0 &= \sum_i - \frac{(T^{(1)}e_i, e_0)(T^{(1)}e_0, e_i)}{(\lambda_i - \lambda_0)^2} e_0 \\
&\quad + \sum_i \left[ - \frac{(T^{(2)}e_0, e_i)}{(\lambda_i - \lambda_0)} + \sum_j \frac{(T^{(1)}e_0, e_j)(T^{(1)}e_j, e_i)}{(\lambda_j - \lambda_0)(\lambda_i - \lambda_0)} \right. \\
&\quad \left. - \frac{(T^{(1)}e_0, e_0)(T^{(1)}e_0, e_i)}{(\lambda_i - \lambda_0)^2} \right] e_i.
\end{aligned} \tag{A19}$$

Based on these formulas, the eigenmode can be readily calculated.

**APPENDIX B: EVALUATION OF  $I_1(m, n)$  AND  $I_2(m, n)$** 

Evaluation of  $I_1(m, n)$ .

$$\begin{aligned}
 I_1(m, n) &= \int_0^L \sqrt{\frac{2}{L}} \sin \left[ \frac{(2n-1)\pi x}{2L} \right] \\
 &\quad \times \left\{ \int_0^x \sqrt{\frac{2}{L}} \sin \left[ \frac{(2m-1)\pi x}{2L} \right] dx \right\} dx \\
 &= \int_0^L \frac{4}{(2m-1)\pi} \left\{ 1 - \cos \left[ \frac{(2m-1)\pi x}{2L} \right] \right\} \\
 &\quad \times \sin \left[ \frac{(2n-1)\pi x}{2L} \right] dx. \quad (B1)
 \end{aligned}$$

By using the simple trigonometric relation  $\sin(\alpha)\cos(\beta) = \frac{1}{2} \sin(\alpha+\beta) + \frac{1}{2} \sin(\alpha-\beta)$ , one finds

$$\begin{aligned}
 I_1(m, n) &= \int_0^L \frac{4}{(2m-1)\pi} \left\{ \sin \left[ \frac{(2n-1)\pi x}{2L} \right] \right. \\
 &\quad \left. - \frac{1}{2} \sin \left[ \frac{(n+m-1)\pi x}{L} \right] \right. \\
 &\quad \left. - \frac{1}{2} \sin \left[ \frac{(n-m)\pi x}{L} \right] \right\} dx, \quad (B2)
 \end{aligned}$$

which can be integrated as

$$I_1(m, n) = \begin{cases} \frac{8L}{(2m-1)^2 \pi^2} & \text{if } n = m, \\ \frac{4L}{(2m-1)\pi^2} \left[ \frac{4}{(2n-1)} + \frac{(-1)^{(n+m-1)} - 1}{(n+m-1)} + \frac{(-1)^{(n-m)} - 1}{(n-m)} \right] & \text{if } n \neq m. \end{cases} \quad (B3)$$

Evaluation of  $I_2(m, n)$ .

Similarly,

$$\begin{aligned}
 I_2(m, n) &= \int_0^L \sqrt{\frac{2}{L}} \sin \left[ \frac{(2n-1)\pi x}{2L} \right] \\
 &\quad \times \left\{ \int_0^x dx \int_0^x \sqrt{\frac{2}{L}} \sin \left[ \frac{(2m-1)\pi x}{2L} \right] dx \right\} dx \\
 &= - \int_0^L \frac{4}{(2m-1)\pi} \sin \left[ \frac{(2n-1)\pi x}{2L} \right] \\
 &\quad \times \left\{ \frac{2L}{(2m-1)\pi} \sin \left[ \frac{(2m-1)\pi x}{2L} \right] - x \right\} dx. \quad (B4)
 \end{aligned}$$

By using the trigonometric relation  $\sin(\alpha)\sin(\beta) = \frac{1}{2} \cos(\alpha - \beta) - \frac{1}{2} \cos(\alpha + \beta)$ , one obtains

$$\begin{aligned}
 I_2(m, n) &= \int_0^L \frac{4L}{(2m-1)^2 \pi^2} \left\{ -\cos \left[ \frac{(m-n)\pi x}{L} \right] \right. \\
 &\quad \left. + \cos \left[ \frac{(m+n-1)\pi x}{L} \right] \right. \\
 &\quad \left. + \frac{(2m-1)\pi}{L} x \sin \left[ \frac{(2n-1)\pi x}{2L} \right] \right\} dx, \quad (B5)
 \end{aligned}$$

which leads to

$$I_2(m, n) = \begin{cases} \frac{4L^2}{\pi^3} \left[ \frac{-\pi}{(2m-1)^2} + \frac{4(-1)^{m+1}}{(2m-1)^3} \right] & \text{if } n = m, \\ \frac{(-1)^{n+1} 16L^2}{(2n-1)^2 (2m-1) \pi^3} & \text{if } n \neq m. \end{cases} \quad (B6)$$

- <sup>1</sup>L. Rayleigh, "On the dynamics of revolving fluids," *Proc. R. Soc. London, Ser. A* **93**, 148 (1916).
- <sup>2</sup>S. Wang and Z. Rusak, "The dynamics of a swirling flow in a pipe and transition to axisymmetric vortex breakdown," *J. Fluid Mech.* **340**, 177 (1997).
- <sup>3</sup>S. Wang and Z. Rusak, "On the stability of an axisymmetric rotating flow in a pipe," *Phys. Fluids* **8**, 1007 (1996).
- <sup>4</sup>F. Gallaire and J.-M. Chomaz, "The role of boundary conditions in a simple model of incipient vortex breakdown," *Phys. Fluids* **16**, 274 (2004).
- <sup>5</sup>A. Garg and S. Leibovich, "Spectral characteristics of vortex breakdown flowfields," *Phys. Fluids* **22**, 2053 (1979).
- <sup>6</sup>T. Mattner, P. Joubert, and M. Chong, "Vortical flow. Part 1: Flow in a constant diameter pipe," *J. Fluid Mech.* **463**, 259 (2002).
- <sup>7</sup>A. Szeri and P. Holmes, "Nonlinear stability of axisymmetric swirling flows," *Philos. Trans. R. Soc. London, Ser. A* **326**, 327 (1988).
- <sup>8</sup>H. B. Squire, "Rotating fluids," in *Surveys in Mechanics*, edited by G. K. Batchelor and R. M. Davies (Cambridge University Press, Cambridge, 1956), pp. 139–161.
- <sup>9</sup>R. R. Long, "Steady motion around a symmetrical obstacle moving along the axis of a rotating liquid," *J. Meteorol.* **10**, 197 (1953).
- <sup>10</sup>F. Gallaire, J.-M. Chomaz, and P. Huerre, "Closed-loop control of vortex breakdown: A model study," *J. Fluid Mech.* **511**, 67 (2004).
- <sup>11</sup>P. Schmid and D. Henningson, *Applied Mathematical Sciences* (Springer-Verlag, New York, 2001), Vol. 142.
- <sup>12</sup>J. Z. Wu, H. Y. Ma, and M. D. Zhou, *Vorticity and Vortex Dynamics* (Springer, Berlin, 2006).
- <sup>13</sup>T. Kato, *Die Grundlehren der Mathematischen Wissenschaften* (Springer-Verlag, New York, 1966), Vol. 132.